UNIVERSITY OF TURKU

QUANTUM COMPLEX NETWORKS

Johannes Nokkala

TURUN YLIOPISTON JULKAISUJA – ANNALES UNIVERSITATIS TURKUENSIS
SARJA - SER. AI OSA - TOM. 595 | ASTRONOMICA - CHEMICA - PHYSICA - MATHEMATICA | TURKU 2018

UNIVERSITY OF TURKU

QUANTUM COMPLEX NETWORKS

Johannes Nokkala

TURUN YLIOPISTON JULKAISUJA – ANNALES UNIVERSITATIS TURKUENSIS
SARJA - SER. AI OSA - TOM. 595 | ASTRONOMICA - CHEMICA - PHYSICA - MATHEMATICA | TURKU 2018

University of Turku

Faculty of Science and Engineering
Department of Physics and Astronomy

Supervised by

Sabrina Maniscalco
Department of Physics and Astronomy
University of Turku
Finland

Jyrki Piilo
Department of Physics and Astronomy
University of Turku
Finland

Reviewed by

Ginestra Bianconi
School of Mathematical Sciences
Queen Mary University of London
United Kingdom

Marco Genoni
Department of Physics
University of Milan
Italy

Opponent

Sougato Bose
Department of Physics and Astronomy
University College London
United Kingdom

ISBN 978-951-29-7467-2 (PRINT)
ISBN 978-951-29-7468-9 (PDF)
ISSN 0082-7002 (Print)
ISSN 2343-3175 (Online)
Grano Oy - Turku, Finland 2018

Acknowledgements

First and foremost, I would like to thank my supervisors Jyrki and Sabrina for being my guides on my journey towards thesis defense. Your foresight and experience, the many ideas and discussions, and your continuous support have been invaluable. I am also deeply greatful for the considerable freedom I've had to pursue my interests, and how even in the busiest of times, you've always had time for me.

I count myself lucky to have been a part of such a warm and friendly work community. In particular, I am grateful for having great office mates throughout my thesis project. When I started in 2014, I was welcomed with open arms and big smiles by the senior PhD students, which immediately made me feel at home and accepted. As years went by and office mates changed, the room I was in eventually became known as "the quiet room", as the occupants all quietly focused on their work. I greatly appreciated this distraction-free atmosphere.

I also wish to thank the many people from outside of my home university that I've had the honor to meet and work with during the thesis project. In particular, I want to thank Bassano, Fernando, Francesco, Giacomo, Guillermo, Nicolas, Rebecca, Roberta, and Valentina. Each of you made important contributions to this thesis project, and I am very proud of how it turned out. I hope our paths will cross again in the future!

While perhaps having little impact on the Thesis contents, the project itself could not have been possible without financial support from Jenny and Antti Wihuri foundation for the first three years, for which I am grateful. I also wish to thank the Department of Physics and Astronomy of the University of Turku for employing me for the final year, during which this Thesis was written.

Throughout my life, my family has been a source of support, encouragement and inspiration. Although I didn't have many opportunities to interact with him directly, what I heard of my grandfather Hokee Minn (cosmology) inspired me to pursue a career in physics. Further sources of

inspiration came from my grandmother Eeva Kangasmaa-Minn (linguistics) and my father Seppo and mother Christina (both genetics). Thanks to the biology department moving to Quantum, the trip to a coffee break with my parents has been short and I've enjoyed many a cup of coffee while discussing science, my thesis project, and life in general. These occasions have been important to me. Finally, I wish to thank the brightest star in my life, Nina. Your love and support have kept me going.

Contents

Abstract

This Thesis focuses on networks of interacting quantum harmonic oscillators and in particular, on them as environments for an open quantum system, their probing via the open system, their transport properties, and their experimental implementation. Exact Gaussian dynamics of such networks is considered throughout the Thesis.

Networks of interacting quantum systems have been used to model structured environments before, but most studies have considered either small or non-complex networks. Here this problem is addressed by investigating what kind of environments complex networks of quantum systems are, with specific attention paid on the presence or absence of memory effects (non-Markovianity) of the reduced open system dynamics. The probing of complex networks is considered in two different scenarios: when the probe can be coupled to any system in the network, and when it can be coupled to just one. It is shown that for identical oscillators and uniform interaction strengths between them, much can be said about the network also in the latter case. The problem of discriminating between two networks is also discussed.

While state transfer between two sites in a (typically non-complex) network is a well-known problem, this Thesis considers a more general setting where multiple parties send and receive quantum information simultaneously through a quantum network. It is discussed what properties would make a network suited for efficient routing, and what is needed for a systematic search and ranking of such networks. Finding such networks complex enough to be resilient to random node or link failures would be ideal.

The merit and applicability of the work described so far depends crucially on the ability to implement networks of both reasonable size and complex structure, which is something the previous proposals lack. The ability to implement several different networks with a fixed experimental setup is also highly desirable. In this Thesis the problem is solved with a proposal of a fully reconfigurable experimental realization, based on map-

ping the network dynamics to a multimode optical platform.

Tiivistelmä

Tämä väitöskirja keskittyy vuorovaikuttavien kvanttimekaanisten harmonisten oskillaattorien muodostamiin verkkoihin ja erityisesti niihin ympäristöinä avoimelle kvanttisysteemille, niiden luotaamisen avoimen systeemin kautta, niiden siirto-ominaisuuksiin, ja niiden kokeelliseen toteutukseen. Väitöskirjassa käsitellään näiden verkkojen eksaktia Gaussista dynamiikkaa.

Vuorovaikuttavien kvanttisysteemien verkkoja on käytetty rakenteellisten ympäristöjen malleina aikaisemmin, mutta usein on käsitelty joko pieniä tai ei-kompleksisia verkkoja. Tässä väitöskirjassa tähän ongelmaan vastataan tutkimalla millaisia ympäristöjä kvanttisysteemien muodostamat kompleksiset verkot ovat, kiinnittäen erityistä huomiota mahdollisiin muistiefekteihin (ei-Markovisuuteen) avoimen systeemin redusoidussa dynamiikassa. Kompleksisten verkkojen luotausta tarkastellaan kahdessa eri tapauksessa: kun luotaimen voi kytkeä mihin tahansa verkon osaan, ja kun sen voi kytkeä vain yhteen. Tullaan näkemään että identtisille oskillaattoreille ja vakiokytkentävoimakkuudelle niiden välillä myös jälkimmäisessä tapauksessa verkosta voi oppia paljon. Lyhyesti tarkastellaan myös onglemaa jossa tutkitaan ovatko kaksi annettua verkkoa samat vai ei.

Tilan siirto verkon kahden osan välillä on tunnettu ongelma. Tässä väitöskirjassa tarkastellaan yleisempää ongelmaa missä useat osapuolet lähettävät ja vastaanottavat kvantti-informaatiota samanaikaisesti kvanttiverkon kautta. Väitöskirjassa pohditaan mitkä ominaisuudet tekisivät verkosta sopivan tämän tehtävän tehokkaaseen toteuttamiseen, ja mitä tarvitaan jotta voitaisiin järjestelmällisesti etsiä ja luokitella verkkoja tätä tarkoitusta varten. Olisi ihanteellista löytää soveliaita verkkoja jotka olisivat riittävän kompleksisia sietääkseen satunnaisia osan tai linkin menetyksiä.

Tähän asti kuvatun työn tärkeys ja soveltuvuus riippuu merkittävällä tavalla kyvystä toteuttaa kokeellisesti verkkoja jotka ovat sekä melko isoja että kompleksisia. Aikaisemmilta kokeellisilta toteutuksilta tämä kyky puuttui. Mahdollisuus toteuttaa useita eri verkkoja samalla koejärjestelyllä

olisi myös erittäin hyödyllistä. Tässä väitöskirjassa tämä puute korjataan antamalla ehdotus nämä ehdot täyttävästä kokeellisesta toteutuksesta joka perustuu verkon dynamiikan kuvaukseen usean moodin optisella alustalla.

List of publications

This Thesis consists of a review of the subject and the following original research articles:

I **Complex quantum networks as structured environments: engineering and probing**,
J. Nokkala, F. Galve, R. Zambrini, S. Maniscalco, J. Piilo, Sci. Rep. **6**, 26861 (2016).

II **Energy backflow in strongly coupled non-Markovian continuous-variable systems**,
G. Guarnieri, *J. Nokkala*, R. Schmidt, S. Maniscalco, B. Vacchini, Phys. Rev. A **94**, 062101 (2016).

III **Non-Markovianity over Ensemble Averages in Quantum Complex Networks**,
J. Nokkala, S. Maniscalco, J. Piilo, Open Syst. Inf. Dyn. **24**, 1740018 (2017).

IV **Reconfigurable optical implementation of quantum complex networks**,
J. Nokkala, F. Arzani, F. Galve, R. Zambrini, S. Maniscalco, J. Piilo, N. Treps, V. Parigi, New J. Phys. **20**, 053024 (2018).

V **Local probe for connectivity and coupling strength in quantum complex networks**,
J. Nokkala, S. Maniscalco, J. Piilo, Sci. Rep. **8**, 13010 (2018).

Chapter 1

Introduction

Quantum mechanics is a non-commutative probabilistic theory concerning measurement results, usually applicable on very small scales, in temperatures near absolute zero, and in other conditions similarly far removed from everyday experience. Since its birth in the beginning of the 20th century, it has interacted with various other branches of formal and natural sciences, often leading to benefits to both quantum and classical sides and even to new subfields within quantum mechanics. Some notable examples include chemistry [1–3] (1920s), special relativity [4–7] (1930s), electrodynamics [8–10] (1950s), optics [11–13] (1960s), information theory [14] (1970s), theoretical computer science [15–17] (1980s), and category theory [18] (2000s). In particular, the application of network theory in the quantum case has seen increasing interest in the 2000s, partly motivated by its successful application in, e.g., statistical physics [19], biology [20] and sociology [21]. Generally speaking, networks are objects composed of discrete subsystems, or nodes, with pairwise connections between them, or links. Today, a plethora of different types of quantum networks have been introduced and applied to problems ranging from the design of large-scale quantum communication networks [22] to quantum computing with graph states [23], and new research on the topic is accumulating at an increasing rate.

In part due to its recency, and in part due to there being neither a unified framework nor a well-structured research community, the study of quantum networks is currently highly fragmented. Indeed, there is no definitive or commonly accepted meaning to the concept "quantum network", but rather research is split between different types of objects that might all be referred to as quantum networks. From the point of view of network science though, this can be seen as natural, since there is no definitive "classical network"

either; airports and flight routes, neurons and synapses, as well as research articles and citations can all be treated as networks. A chapter in this Thesis has been reserved for covering relevant concepts in graph and network theory and for a brief introduction to some common types of quantum networks and their applications, as well as to other research avenues that could perhaps be said to fall under the umbrella of quantum network science.

A particular, straightforward way to introduce the concept of a network in the quantum case is to take a set of pairwise interacting quantum systems and identify the systems as nodes and the interaction terms as links. Often, one may start from a matrix representation of a graph and construct from it the Hamiltonian of the corresponding quantum network in a step-by-step fashion. Networks of interacting fermions are a notable example, typically derived from either the adjacency or the Laplace matrix of a graph. They have been considered, e.g., in the context of quantum walks [24], quantum computing [25], perfect state transfer [26], and more general transport problems when considering dissipative networks as models for biomolecules [27, 28]. Bosonic quantum networks, on the other hand, have been used to model structured environments for an open quantum system [29] and for the study of collective phenomena such as synchronization [30] in the case of open quantum networks immersed in a heat bath. When the quantum network is of reasonable size and non-regular structure, it is said to be a (quantum) complex network.

The main focus of this Thesis is the study of complex networks of interacting quantum harmonic oscillators, and in particular their exact Gaussian dynamics. The topics considered can be captured by the following research questions. In the framework of open quantum systems, what kind of environments are these networks? What can we say about the network if we use a controllable open quantum system as a probe? Can we use networks to transport and route quantum information and entanglement, and if yes, which networks are best? How could one experimentally implement networks with reasonable size and complex structure? The answers to these questions, provided in part in this Thesis, pave the way to further studies of quantum complex networks both in theory and experimentally.

The rest of this Thesis is organized as follows.

Chapter 2: Relevant concepts from graph and network theory are presented. Quantum networks are introduced and the motivations to study them are discussed.

Chapter 3: The definition of the quantum network considered in this Thesis is given and the theoretical tools applied in its study in later chapters are presented.

Chapter 4: Quantum networks are studied as tunable environments for an open quantum system, covering related results from Publications I-III.

Chapter 5: The probing of quantum networks is considered in two different scenarios, covering results from Publications I and V. Additionally, the network discrimination problem is introduced and discussed.

Chapter 6: Transport of quantum information in networks is considered (Publication III). The routing problem is introduced and routing capacity of a quantum network discussed (upcoming work).

Chapter 7: The requirements to experimentally implement quantum networks are discussed. The proposal for an optical reconfigurable implementation of quantum complex networks from Publication IV is presented.

Chapter 8: The contents of the Publications I-V are summarized. The merit and limitations of the research, as well as remaining open questions and possible future research avenues are discussed.

Chapter 2

Motivation for quantum networks

The first two Sections of this Chapter are intended to provide a compact review of the relevant concepts from graph and network theory, respectively. While the terms graph and network are sometimes used interchangeably, in this Thesis graph is taken to be an abstract mathematical object, while network is taken to be a physical system that can be represented by a graph. In particular, it is discussed what makes a network complex. The final Section discusses what makes a network quantum, and provides a brief overview on commonly used quantum networks and their applications, as well as closely related topics, to exemplify the reasons to study such networks.

This Chapter, especially the first two Sections, is heavy with terminology. To aid the reader, a concept defined for the first time is emphasized with *italic font*. Central concepts are given as **Definitions**. **Remarks** are used to further clarify how the concepts introduced here relate to Thesis contents. Here, the conventions in the books *Introduction to Graph Theory* by Robin J. Wilson [31] and *Networks: an introduction* by Mark Newman [32] are followed, unless stated otherwise. These books are also recommended for an interested reader for proper development of the reviewed material.

At variance, to the best of the author's knowledge, no such comprehensive treatise exists for quantum networks, see however Refs. [33, 34] and the references therein. Monographs focusing on specific types of quantum networks have been written, and when applicable, they are mentioned when the corresponding networks are introduced.

2.1 Graph theory

Graph theory is a branch of mathematics concerned with the study of graphs. This Thesis focuses on networks represented by simple graphs, defined as follows.

Definition 1. *A simple graph is a pair $G = \{V, E\}$, where V is a non-empty finite set of elements called vertices, and E is a finite set of unordered pairs of distinct vertices, called edges.*

While vertices are also commonly called nodes or points and edges links or lines, this Thesis consistently uses vertices and edges for graphs, and nodes and links for networks. Furthermore, all graphs will be simple unless stated otherwise. An example of a simple graph is shown in Fig. 2.1.

Let V_G and E_G be the vertex and edge sets of some simple graph G. A vertex $v \in V_G$ is said to be *incident* to an edge $e \in E_G$ iff $e = \{v, m\}$, often abbreviated to $e = vm$, for some $m \in V_G$. Notice that vm and mv are the same edge. The presence of such an edge in G makes the vertices v and m *adjacent*. The total number of vertices adjacent to v is called its *degree*. A vertex of degree 0 is said to be an *isolated vertex*, while a vertex that is adjacent to all other vertices of G is said to be a *dominating vertex*. Sometimes vertex labels are unimportant and are dropped. The difference between labelled and unlabelled graphs can matter for example when enumerating them.

The edge vm is said to be *incident* to both vertex v and vertex m. If $vm, vu \in E_G$, because of the common vertex v the edges vm and vu are called *adjacent*. The edges of a graph can be *weighted*, typically using a function $w : E_G \to \mathbb{R}_+$, but certain quantum states can be quite naturally represented by graphs with weights in $\mathbb{C}$, as will be seen.

A sequence of adjacent vertices in which all elements are distinct is called a *path*. The number of edges a path traverses is its *length*. The *distance* between two vertices is the length of the shortest path that begins with one and ends with the other; if no such path exists, the distance is defined to be infinite. In this Thesis, a path is said to be *closed* if the first and last elements are adjacent. The sequence of adjacent edges induced by a path may also be considered a path, as can be the corresponding alternating sequence of adjacent vertices and edges.

In this Thesis, the number of vertices in a graph is called its *size*, denoted by N, while the number of edges is denoted by M. The *degree sequence* of a

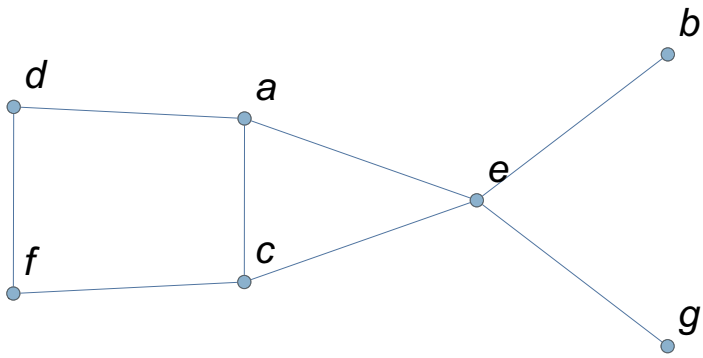

Figure 2.1: An example of a simple graph with seven labelled vertices (points) and eight edges (lines).

graph is the sequence of degrees of each vertex in the graph; a graph where all vertices have the same degree is called *regular*. If the constant degree is r, the graph is also called *r-regular*. A graph is said to be *connected* if for any distinct pair of vertices $v, m \in V_G$, there is a path $\{v, \ldots, m\}$ in G; informally speaking, connected graphs are in one piece, like the graph in Fig. 2.1 is. Otherwise, the graph is said to be *disconnected*. This Thesis focuses on connected graphs. Two graphs G and H are said to be *isomorphic* if there exists a bijection $\alpha : V_G \to V_H$ such that $uv \in E_G \Rightarrow \alpha(u)\alpha(v) \in E_H$ for all vertices $u, v \in V_G$. In this Thesis, isomorphic graphs are treated as identical. The concept of isomorphic graphs allows one to define *graph invariants*, often simply called graph properties: they are any functions f of graphs such that $f(G_1) = f(G_2)$ whenever G_1 and G_2 are isomorphic. Size, degree sequence, and being connected are all examples of graph invariants.

With paths and connectedness defined, one is now in a position to define *path graphs*, which are connected graphs that are their own longest path, and *tree graphs*, which are connected graphs where all paths are open. Clearly, both types of graphs have exactly $N - 1$ edges, and in fact, path graphs are a special case of tree graphs. Two graph invariants of particular interest when studying how well a graph is connected are called *edge-connectivity* and *vertex-connectivity*, which are the minimum number of edges and vertices, respectively, the deletion of which results in a disconnected graph. Both quantities are equal to one for all path and tree graphs,

making them minimal connected graphs.

Remark. This Thesis focuses on quantum networks naturally represented by connected weighted simple graphs, and in particular ones represented by both path and tree graphs are considered, alongside more complicated graphs.

As working with abstract graphs can be cumbersome, in practice various representations are used and no distinction is made between a graph and one of its representations. Naturally, graph invariants are independent of a particular representation.

An often seen representation of a graph is a *plane figure*, where each vertex is drawn for example as a point or a circle, and for each edge a line or a curve is drawn between the corresponding vertices. What is shown in Fig. 2.1 is a plane figure of the graph G with $V_G = \{a, b, c, d, e, f, g\}$ and $E_G = \{ac, ad, ae, be, ce, cf, df, eg\}$.

Matrix representations are also commonplace. They are not only convenient when working with graphs on a computer, but also essential in the study of spectral graph theory, which is concerned with the interplay between a graph's structure and the eigenvalues of its matrix representations. In Chapter 5, results from spectral graph theory are used to develop a probing scheme applicable to quantum networks. In this Thesis, two matrix representations are used: the (weighted) *adjacency matrix* $\mathbf{V}$ is the $N \times N$ matrix with elements $\mathbf{V}_{ij} = w(ij)$ if $ij \in E_G$ and $\mathbf{V}_{ij} = 0$ otherwise; and the (weighted) *Laplace matrix*, which is the $N \times N$ matrix $\mathbf{L} = \mathbf{D} - \mathbf{V}$ where the diagonal matrix $\mathbf{D}$ has elements $\mathbf{D}_{ii} = \sum_{j=1}^{N} \mathbf{V}_{ij}$. Notice that the case of unweighted graphs is recovered by setting $w(ij) = 1$ for all $ij \in E_G$, in which case the elements of the matrix $\mathbf{D}$ are just the vertex degrees.

Remark. While the quantum networks focused on in the Thesis are derived from the Laplace matrix, they may also be described in terms of the adjacency matrix. While the network Hamiltonian remains unchanged, sometimes it can be more convenient to consider one matrix over the other; for instance, the network parameters might have a somewhat simpler form.

Simple graphs can be generalized in several ways. For example, one may consider *directed graphs*, where E_G consists of ordered pairs of vertices, graphs with *loops*, where edges are allowed to contain the same vertex

twice, graphs with *multi-edges*, where E_G is allowed to be a multiset, i.e. it may contain duplicate elements, and *infinite graphs*, where V_G and E_G are allowed to contain infinitely many elements.

2.2 Network theory

In short, network theory is concerned with graphs as a representation of networks, the networks themselves, the mechanisms that give the existing networks their structure, and dynamical processes on networks. While there is some overlap with graph theory, network theory has a greater emphasis on empirical studies. The graph terminology introduced in the previous Section is inherited by networks, with the exception that in this Thesis, networks are said to be composed of nodes and links, rather than vertices and edges. As network theory is interdisciplinary, there is no universally adopted definition of a network. In this Thesis, the following loose definition is used.

Definition 2. *A network is a physical system well-represented by a graph.*

For a system to be amenable to such a presentation, it should be possible to partition it into discrete subsystems with pairwise connections; whether this is worthwhile is a separate matter. It should be kept in mind that fixing a set of subsystems (classical or otherwise) to be the nodes of a network does not by any means define a unique network. An illustrative example of this from Ref. [35] considers a set of people and auxiliary data on them that could be used to construct the links of a network. Choosing to make closely related people adjacent and choosing to make people with the same first name adjacent will surely give rise to two very different networks, of which only one could conceivably be useful!

The pertinent concept is, of course, the complexity of a network. Very loosely speaking, a *complex network* is "real network-like", meaning that it has structural properties often observed in data collected on, for example, how routers are connected on the Internet, or how scientific articles cite each other, or how individuals are acquainted. More formally, real networks are often observed to be approximately *scale-free*, *small-world*, and have a high *transitivity*[1].

[1]Notice that a given complex network is not necessarily all of these. While further

In a random network where each link is equally likely to exist, it is well known that degrees tend to be close to the mean degree, which then serves as an internal scale. At variance, a network is said to be scale-free if in principle arbitrarily large deviations from the mean can exist. It is known that networks where the distribution of node degrees follows a power-law with an exponent between 2 and 3 are scale-free [36]. *Diameter* is defined to be the maximum distance in a network or graph. The small-world property refers to a network having a diameter proportional to the logarithm of its size, making such networks significantly more efficient to navigate than random networks. Finally, transitivity in this context refers to transitivity of nodes being adjacent, and is typically measured by the *clustering coefficient*, defined to be the probability that two random neighbors of a random node of degree at least two are also themselves adjacent, i.e. it is the fraction of closed paths of length two to all paths of length two.

Remark. In this Thesis, and in particular in the case of quantum networks, a network is said to be complex if it is of reasonable size and not a lattice, i.e. not a regular graph with translational symmetry. For example, while the graph in Fig. 2.1 is not a lattice, it might be considered too small to be called complex. While some of the networks that will be studied in later Chapters are not real network-like, hence perhaps not complex from the point of view of network theory, they will nevertheless be considered complex for quantum networks.

In particular, networks based on graphs generated by commonly used random graph models are considered. An Erdős-Rényi (ER) random graph refers to a graph generated by either of two closely related models: in the $G(N, p)$ model, each possible edge between the N vertices will be selected with a probability p, while in the $G(N, M)$ model, a graph is drawn uniformly at random from the distribution of all graphs with exactly N vertices and M edges. In this Thesis, the $G(N, p)$ model is used unless stated otherwise. A Barabási-Albert (BA) random graph $G(N, K)$ is constructed starting from a connected graph of three vertices, and iteratively adding a new node with K edges until the graph has N vertices, connecting the new edges to vertices with a probability proportional to their degree. Finally, a Watts-Strogatz (WS) random graph $G(N, k, p)$ is constructed starting from

properties associated with complex networks exist, the three mentioned here are perhaps most well-known.

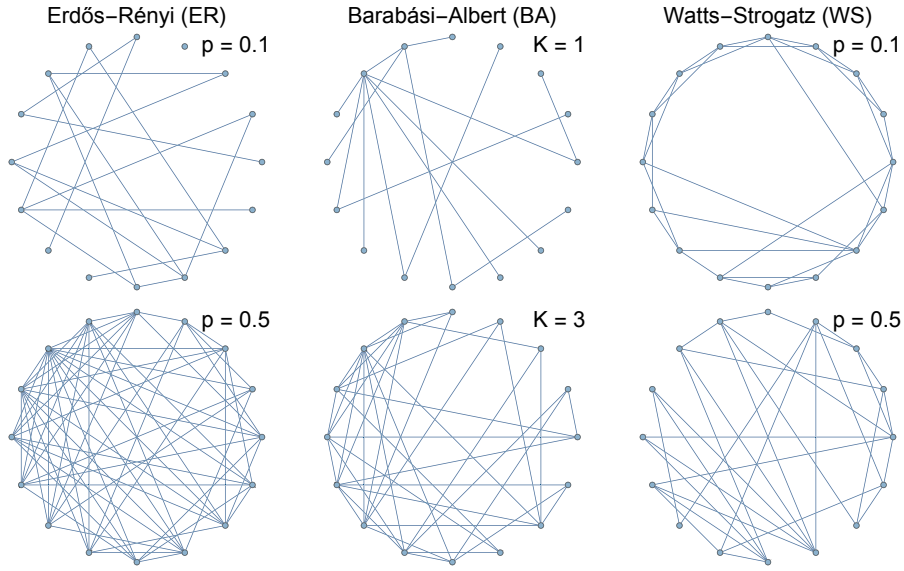

Figure 2.2: Examples generated using the three random graph models considered in this Thesis. Each column corresponds to one of the models. In ER random graphs, each possible edge is selected independently with probability p. In a BA random graph, each new vertex is connected to K old ones with a probability proportional to their degrees, which tends to lead to some nodes having a very high degree. A WS random graph is constructed starting from a $2k$-regular circular graph, after which each edge is rewired independently with probability p. Here, a fixed value $k = 2$ has been used.

a circular regular graph of N vertices connected to $k-$th nearest neighbors and rewiring each edge randomly with a probability p. All three models are illustrated in Fig. 2.2.

Each of these models has played an important role in graph and network theory. ER random graph model was the first attempt to consider statistical properties of large graphs, and is still used today to, e.g., argue that finding a given vertex of a graph by quantum walk is optimal for almost all graphs [37]. It is well known that real networks are, in fact, rarely congruent with the ER random graph model, as ER random graphs are neither scale-free nor small-world, and have low transitivity. This problem motivated the introduction of the BA and WS models.

The former can be used to generate scale-free graphs with a small diameter, but BA random graphs have low transitivity. On the other hand, at very low values of the rewiring probability p and for $k \geq 2$, WS random graphs have a high number of closed paths of length two and hence high transitivity, but also high diameter. Transitivity decreases much more slowly than the diameter as p is increased, leading to a regime of parameter values where WS random graphs are both small-world and transitive. At the other extreme of $p \lesssim 1$, WS random graphs are effectively random. While it can therefore be said that the WS model interpolates between regular and random graphs with complexity appearing in between, it cannot produce scale-free graphs.

2.3 Quantum networks

All quantum systems of interest that are composed of pairwise related discrete subsystems can be quite naturally described in terms of graphs, which can sometimes lead to a particularly elegant and compact description. This is in part what makes the introduction of concepts from graph and network theory to the quantum case appealing. Given the diversity of objects that may all be said to be quantum networks, it seems unlikely that any precise definition covering all of them could be introduced. Therefore, this Thesis will settle for the following loose definition analogous to that of classical networks. It should be stressed that the definition, by design, allows some parts of the network to be classical. This allows one to, e.g., include the devices storing the quantum systems playing the role of nodes as part of the network.

Definition 3. *A quantum network is a physical system that requires a quantum description and is well-represented by a graph.*

One might quite reasonably ask if a network fulfilling this definition is guaranteed to be quantum in the sense that its observable behaviour cannot be emulated by any classical mechanism. The short answer is that there is no such guarantee. Like with classical networks, links of a quantum network should be chosen with a specific application in mind, and in general, multiple choices might be available as will be seen. What gives the network its quantumness is then determined on a case by case basis. While this might seem unsatisfactory, to find a universal quantifier of the

quantumness of a network seems to be nearly as difficult as finding one for general quantum systems as networks are ubiquitous. Naturally, of greatest interest are exactly the networks that have properties or applications that no classical networks can have.

The following brief overview is not intended to be exhaustive, but rather just illustrate the concept of quantum networks with some specific examples and discuss what makes them quantum and the motivations of studying them. Some closely related research avenues lying in the intersection of graph and quantum theory are also presented.

Classification and applications

In *state-based quantum networks*, a graph is used to represent a state of a compound quantum system. For example, nodes can be (possibly multiple) quantum systems and links entanglement. When states are considered to be equivalence classes of initial state preparations, the graph can be interpreted as a representation of the (preparatory stage or full) experiment. The quantumness (or lack thereof) of the state is inherited by the network. Treatises on the networks themselves appear to be scarce, however one might find, e.g., Chapter 3 of [38] or Refs. [23, 39] useful.

The networks used as an initial resource in measurement-based quantum computing are multimode highly entangled states, called *cluster states* or *graph states*[2]. Computation consists of local measurements and local operations on the state, with final measurement result yielding the outcome of the computation. As the state is consumed in the process, this scheme is also known as one way quantum computing. Another application of graph or cluster state formalism is to construct a graphical calculus of quantum dynamics, where (a restricted class of) quantum operations are faithfully represented by transformations on the graph; such an approach has been used to simulate the action of so-called stabilizer circuits on a registry of n qubits with typically only a quasi-linear $\mathcal{O}(n \log(n))$ scaling of time and memory [40]. Continuous-variable cluster states, as opposes to their qubit counterparts, can be prepared deterministically but are only approximate cluster states, as ideal cluster states would require infinite squeezing. In [41], a graphical calculus is proposed for such non-ideal cluster states, where the states are represented by graphs with loops and edge weights in $\mathbb{C}$.

[2]The exact definition of either is context-dependent; the concepts are synonyms to some authors while different for others.

In *Hamiltonian-based quantum networks*, a graph is used to represent the Hamiltonian of a compound quantum system. For example, nodes can be quantum systems and links interaction terms. Often one may construct the network Hamiltonian directly from the matrix representation of a graph. The quantumness of these networks is harder to directly quantify but could be linked to, e.g., the quantumness of a random walk on the network [42], or the ability of the network to generate entanglement between external systems in contact with it [30]. As universal quantum computation can be implemented as a quantum walk [25], this might offer yet another avenue to quantify the network quantumness. As long as hermiticity of the Hamiltonian is preserved, edge weights in $\mathbb{C}$ can also be considered for these quantum networks. In some cases this can make the flow of quantum information through the links biased in such a way that the links in the network can be considered to be directed [43, 44]. Ref. [45] is a treatise focusing on state transfer on such networks, while in [46], these networks are considered in the context of solid state physics and in the presence of environmental noise.

Aside from quantum walks on them, such networks have been studied in the context of transfer of quantum information or excitations from a node to another. Research on perfect state transfer has focused on networks not in contact with an environment, while the presence of an environment is often considered when the networks are used to model bio-molecules in the search for clues to the very high efficiency of photosynthesis in biological complex systems [27, 28]. It has also been suggested that the latter line of research could lead to advances in the design of devices harvesting energy from sunlight [47]. Fundamental research on such networks deals with topics such as probing the networks [29, 48–51].

Remark. The quantum networks focused on in this Thesis are Hamiltonian-based. It will be seen that their Hamiltonians are quadratic, and as such they are naturally represented by simple graphs.

In *channel-based quantum networks*, nodes are capable of receiving, processing and transmitting quantum information, while links are quantum channels. Such nodes are sometimes called quantum processors. The graph can be considered to be a representation of the quantum communication network consisting of the nodes and channels. The quantumness of these networks is due to the non-vanishing quantum capacity of the channels and the ability of the nodes to put this capacity to good use. Ref. [52] is a recent

monograph on the topic with an emphasis on the network aspect, while [53] focuses on the cavity-based approach and the experimental implementation of the nodes.

The construction of these quantum networks has been the subject of steadily increasing research effort in, e.g., China [54–56], as they are a key requirement both in carrying out quantum information processing protocols over vast distances [57] and distributed quantum computing, where a suitable quantum computation is split between several quantum processors [58], or where quantum information is transmitted between local and cloud quantum processors [59]. As the size of these networks grow, it may be expected that aspects from network theory dealing with efficient navigation and fault tolerance in networks become relevant also for them.

It should be stressed that there is overlap between the classes of quantum networks introduced so far. For instance, depending on, e.g., the initial state, the interaction terms in the Hamiltonian might lead to nontrivial correlation structure in the state. A good example of this is the recent proposal for adiabatic preparation of continuous variable cluster states [60], where Hamiltonians with cluster states as ground states are constructed. On the other hand, a channel-based quantum network might be used to set up a large network of entangled states.

Further types of quantum networks could include, for instance, quantum neural networks [61], quantum feedback networks [62], or communication networks with both classical and quantum cryptography protocols. The latter type of networks could be considered as a single network with a quantum and a classical layer, which would make them an example of *multiplex networks*, i.e networks characterized by multiple layers with the same set of nodes but different links. Future quantum computers might also need to process both quantum and classical information in such a way that the two layers could be naturally seen as part of a single multiplex network.

Related topics

Areas of research strongly related to quantum networks include the introduction and study of graph invariants that are partially or fully quantum, the application of graph theory to quantum problems, and the application of quantum theory to graph theoretic problems.

In [63], a phase transition called entanglement percolation is predicted

when considering distribution of entanglement in quantum networks and classical percolation theory, while in [42] a quantifier of the difference between quantum and classical random walk on a graph is introduced, based only on the graph structure. The so-called quantum chromatic number comes in many variants [64], but all are upper bounded by the classical chromatic number. A graph invariant for graph states with inputs and outputs, called flow condition, is introduced in [65]. When satisfied, it guarantees globally deterministic behavior of a class of measurement patterns defined over them. Local unitary equivalence between graph states [66], on the other hand, is of interest in trying to better understand the role of entanglement in computational advantage over classical algorithms.

Introducing concepts from graph theory to quantum problems can be as simple as searching for useful instances of a model by classifying them with graph theory. An example of this is that graphs with low vertex-connectivity and certain additional spectral properties are efficiently controllable [67]. Some formulations of state-based quantum networks naturally inherit theorems from graph theory which may be interpreted in a novel setting, such as Hall's marriage problem rephrased in the language of entangled pair creation in quantum experiments [68]. A straightforward application is to use known results concerning the eigenvalues of graph matrices on, e.g., transfer problems on graphs [69].

Quantum algorithms designed to solve graph theoretic problems intractable with classical algorithms are a paradigmatic example of quantum theory benefitting graph theory. Such algorithms have been introduced for, e.g., vertex matching [70], vertex coloring [71], Betti numbers [72] and finding the maximal clique [73], just to name a few.

Chapter 3

Networks of quantum harmonic oscillators

The purpose of this Chapter is to introduce on the one hand the quantum networks considered in this Thesis, and on the other hand the (quantum side of the) theoretical framework used to study them in the attached Publications. After a short Section on technical details, the quantum network is defined. To study these networks, one should be able to determine their dynamics and have a framework for the classification of the properties given by their Hamiltonian. This is accomplished with multimode Gaussian states formalism and selected tools from open quantum systems theory, respectively. Both topics are briefly reviewed in the last two Sections of this Chapter; for a more in-depth treatment, see, e.g., Ref. [74] for Gaussian dynamics and Refs. [75, 76] for open quantum systems theory.

3.1 On notation and conventions

This Thesis adopts such units that the reduced Planck constant $\hbar = 1$ and the Boltzmann constant $k_\mathrm{B} = 1$. Oscillators have unit mass, unless stated otherwise. Arbitrary units are used for other quantities such as frequency and coupling strength.

Vectors and matrices are denoted by bold symbols. Vectors are column vectors by default. Vectors and matrices can have operators as their elements. Let $\mathbf{x}$ be a matrix of operators $\mathbf{x}_{ij} = x_{ij}$. Then transpose, adjoint and expectation value are defined as $(\mathbf{x}^\top)_{ij} = x_{ji}$, $(\mathbf{x}^\dagger)_{ij} = x_{ij}^\dagger$ and $\langle \mathbf{x} \rangle_{ij} = \langle x_{ij} \rangle$, respectively, i.e. the transpose is applied only to the indices and adjoint and expectation value only to the elements.

In the rest of this Thesis, diagonal matrices are consistently denoted by $\mathbf{\Delta}$, except for the identity matrix, which is denoted by $\mathbf{I}$. A diagonal matrix with elements $\mathbf{\Delta}_{ii} = \mathbf{x}_i$, where $\mathbf{x}^\top = \{x_1, x_2, \dots\}$, is denoted by $\mathbf{\Delta}_\mathbf{x}$. Naturally, powers of such matrices, e.g., $\mathbf{\Delta}_\mathbf{x}^n$, have diagonal elements $\{x_1^n, x_2^n, \dots\}$.

Let $\mathbf{a}^\top = \{a_1, \dots, a_m\}$ and $\mathbf{b}^\top = \{b_1, \dots, b_m\}$ be two vectors of operators. Following Ref. [41], the commutator between $\mathbf{a}$ and $\mathbf{b}$ is defined to be the matrix

$$[\mathbf{a}, \mathbf{b}^\top] = \mathbf{a}\mathbf{b}^\top - (\mathbf{b}\mathbf{a}^\top)^\top,$$

with elements $[\mathbf{a}, \mathbf{b}^\top]_{ij} = [a_i, b_j] = a_i b_j - b_j a_i$. The corresponding anticommutator is defined analogously as

$$[\mathbf{a}, \mathbf{b}^\top]_+ = \mathbf{a}\mathbf{b}^\top + (\mathbf{b}\mathbf{a}^\top)^\top,$$

and it has elements $[\mathbf{a}, \mathbf{b}^\top]_{+ij} = [a_i, b_j]_+ = a_i b_j + b_j a_i$.

3.2 Definition of the quantum network

Consider a simple weighted graph on N vertices represented by a Laplace matrix $\mathbf{L}$. The corresponding network of quantum harmonic oscillators is defined to be the one found by replacing each vertex with a unit mass quantum harmonic oscillator and each edge with a spring-like interaction term with a magnitude given by the weight of the edge. The bare frequencies of the oscillators can be chosen independently of $\mathbf{L}$[1]. Throughout the rest of this Thesis, such networks are referred to simply as quantum networks. Their Hamiltonian, quadratic in momentum and position operators, is

$$H_E = \frac{\mathbf{p}^\top \mathbf{p}}{2} + \mathbf{q}^\top \mathbf{A} \mathbf{q}, \tag{3.1}$$

[1]While the bare frequencies may be interpreted as loops, $\mathbf{L}$ remains by definition invariant if loops are added. Because of this and the useful properties of the spectrum of $\mathbf{L}$, the graph is considered simple and the bare frequencies separate from it.

where the vectors of position and momentum operators read $\mathbf{q}^\top = \{q_1, ..., q_N\}$ and $\mathbf{p}^\top = \{p_1, ..., p_N\}$, and where $\mathbf{A} = \mathbf{\Delta}^2_{\boldsymbol{\omega}}/2 + \mathbf{L}/2$. Here,

$$q_j = \frac{a_j^\dagger + a_j}{\sqrt{2\omega_j}}, \quad p_j = i\sqrt{\frac{\omega_j}{2}}(a_j^\dagger - a_j), \tag{3.2}$$

satisfying the commutation relation $[q_j, p_l] = i\delta_{jl}$, and $\mathbf{\Delta}_{\boldsymbol{\omega}}$ is a diagonal matrix of oscillator frequencies $\boldsymbol{\omega}^\top = \{\omega_1, \ldots, \omega_N\}$. The springlike interaction terms are of the form $w(ij)(q_i - q_j)^2/2$, where $w(ij)$ is the weight of the link ij; in the Hamiltonian (3.1), the interaction terms have been expanded and terms of the form q_i^2 have been absorbed to the free Hamiltonians of the oscillators. Matrix $\mathbf{A}$ may also be written in terms of the graph adjacency matrix $\mathbf{V}$ as $\mathbf{A} = \mathbf{\Delta}^2_{\tilde{\boldsymbol{\omega}}}/2 - \mathbf{V}/2$, where $(\mathbf{\Delta}^2_{\tilde{\boldsymbol{\omega}}})_{ii} = \tilde{\omega}_i^2 = \omega_i^2 + \sum_{j\neq i} \mathbf{V}_{ij}$. Here, the elements of $\tilde{\boldsymbol{\omega}}$ are the effective frequencies resulting from the springlike interaction terms.

General quadratic Hamiltonians are of the form $H = \mathbf{x}^\top \mathbf{M} \mathbf{x}$, where the vector $\mathbf{x}$ contains both the position and momentum operators and $\mathbf{M}$ is a $2N \times 2N$ matrix such that H is Hermitian. They can be diagonalized to arrive at an equivalent picture of uncoupled oscillators provided that $\mathbf{M}$ is positive definite [77]. Since H is Hermitian, this is equivalent with the positivity of the eigenvalues of $\mathbf{M}$, ensuring that the uncoupled oscillators will have real frequencies. In particular, since $\mathbf{A}$ is real and symmetric, the Hamiltonian (3.1) may be diagonalized with an orthogonal matrix $\mathbf{K}$ such that $\mathbf{K}^\top \mathbf{A} \mathbf{K} = \mathbf{\Delta}$. Here the diagonal matrix $\mathbf{\Delta}$ holds the eigenvalues of $\mathbf{A}$ which are guaranteed to be positive as $\mathbf{A}$ is the sum of a positive semidefinite matrix $\mathbf{L}$ and the positive definite matrix $\mathbf{\Delta}_{\boldsymbol{\omega}}$. By defining new operators

$$\mathbf{Q} = \mathbf{K}^\top \mathbf{q}, \quad \mathbf{P} = \mathbf{K}^\top \mathbf{p}, \tag{3.3}$$

and a diagonal matrix $\mathbf{\Delta}_{\boldsymbol{\Omega}} = \sqrt{2\mathbf{\Delta}}$ with elements $\boldsymbol{\Omega}_i = \Omega_i$, the diagonal form of H_E reads

$$H_E = \frac{\mathbf{P}^\top \mathbf{P}}{2} + \frac{\mathbf{Q}^\top \mathbf{\Delta}^2_{\boldsymbol{\Omega}} \mathbf{Q}}{2} = \sum_i^N (P_i^2 + \Omega_i^2 Q_i^2)/2, \tag{3.4}$$

which is the Hamiltonian of N decoupled oscillators with frequencies $\mathbf{\Omega}$. The uncoupled oscillators are also called eigenmodes and their frequencies $\mathbf{\Omega}$ eigenfrequencies.

Physical systems that could naturally have a Hamiltonian of the form (3.1) are discussed in Section 2.3 of Publication III, while general aspects of experimental implementation are discussed in Chapter 7. The final Section of Chapter 7 introduces the main result of Publication IV, namely a proposal for an experimental implementation of quantum networks based on mapping H_E to a multimode optical platform. At the level of Hamiltonians, the mapping means that H_E should be expressed in terms of the vectors $\mathbf{q}'$ and $\mathbf{p}'$ of quadrature operators of the electromagnetic field[2]. The vectors are related to $\mathbf{q}$ and $\mathbf{p}$ as

$$\mathbf{q} = \sqrt{\mathbf{\Delta}_{\boldsymbol{\omega}}^{-1}}\mathbf{q}', \quad \mathbf{p} = \sqrt{\mathbf{\Delta}_{\boldsymbol{\omega}}}\mathbf{p}', \tag{3.5}$$

and the Hamiltonian (3.1) in terms of them reads

$$H_E = \frac{\mathbf{p}'^{\top}\mathbf{\Delta}_{\omega}\mathbf{p}'}{2} + \mathbf{q}'^{\top}\sqrt{\mathbf{\Delta}_{\omega}^{-1}}\mathbf{A}\sqrt{\mathbf{\Delta}_{\omega}^{-1}}\mathbf{q}'. \tag{3.6}$$

Following the steps leading to the diagonal form (3.4), the quadrature operators of the normal modes may be expressed in terms of matrix $\mathbf{K}$ as

$$\mathbf{Q}' = \sqrt{\mathbf{\Delta}_{\Omega}}\mathbf{K}^T\sqrt{\mathbf{\Delta}_{\omega}^{-1}}\mathbf{q}', \quad \mathbf{P}' = \sqrt{\mathbf{\Delta}_{\Omega}^{-1}}\mathbf{K}^T\sqrt{\mathbf{\Delta}_{\omega}}\mathbf{p}', \tag{3.7}$$

and in terms of them, Eq. (3.6) reads

$$H_E = (\mathbf{P}'^{\top}\mathbf{\Delta}_{\mathbf{\Omega}}\mathbf{P}' + \mathbf{Q}'^{\top}\mathbf{\Delta}_{\mathbf{\Omega}}\mathbf{Q}')/2 = \sum_i^N \Omega_i(P_i'^2 + Q_i'^2)/2. \tag{3.8}$$

Before concluding this Section, it should be mentioned that besides the one used in this Thesis, other coupling schemes may be considered in an oscillator network, such as oscillators in the rotating wave approximation,

[2]Unlike elsewhere in this Thesis, in Publication IV $\mathbf{q}'$ and $\mathbf{p}'$ are vectors of position and momentum operators and $\mathbf{q}$ and $\mathbf{p}$ vectors of quadrature operators.

where terms that are not energy conserving are neglected. This leads to position-position as well as momentum-momentum coupling terms in the Hamiltonian, as seen in, e.g., [78]. As such a Hamiltonian may still be diagonalized, it may be expected that much of the results introduced in this Thesis could still apply with some appropriate modifications.

3.3 Gaussian quantum dynamics

Gaussian states, to be defined properly in a moment, are an important class of states in continuous variable quantum information science. The practical reason behind focusing on Gaussian states for the networks is twofold: on the one hand quadratic Hamiltonians like Hamiltonian (3.1) preserve the Gaussianity of an initial Gaussian state during evolution, and on the other hand such dynamics can be efficiently and exactly computed, as will be seen in this Section. The natural initial state for an environment is also Gaussian, so it can be said that such a restriction presents little loss of generality for the study of quantum networks as environments.

Let $\mathbf{x} = \{x_1, \ldots, x_N, p_1, \ldots, p_N\}$ be the $2N$ vector containing the position and momentum operators of the network. The commutation relations will now give rise to a $2N \times 2N$ matrix $\mathbf{J}$ through the relation

$$[\mathbf{x}, \mathbf{x}^\top] = i\mathbf{J}, \tag{3.9}$$

where

$$\mathbf{J} = \begin{pmatrix} 0 & \mathbf{I}_N \\ -\mathbf{I}_N & 0 \end{pmatrix} \tag{3.10}$$

and $\mathbf{I}_N$ is the $N \times N$ identity matrix.

Since $\mathbf{J}\mathbf{J}^\top = \mathbf{I}$, $\mathbf{J}$ is invertible. As it is also skew-symmetric, i.e. $\mathbf{J}^\top = -\mathbf{J}$, it is an example of a so-called symplectic form. Let now $\mathbf{y} = \mathbf{S}\mathbf{x}$, where $\mathbf{S}$ is a real $2N \times 2N$ matrix. Requiring that this transformation preserves the commutation relations (3.9) leads to

$$i\mathbf{J} = [\mathbf{y}, \mathbf{y}^\top] = [\mathbf{S}\mathbf{x}, (\mathbf{S}\mathbf{x})^\top] = \mathbf{S}[\mathbf{x}, \mathbf{x}^\top]\mathbf{S}^\top = i\mathbf{S}\mathbf{J}\mathbf{S}^\top, \tag{3.11}$$

that is to say the matrix must satisfy the condition $\mathbf{S}\mathbf{J}\mathbf{S}^\top = \mathbf{J}$. When this is the case, the matrix is said to be a symplectic matrix (with respect to the symplectic form $\mathbf{J}$). As commutation relations are preserved in unitary evolution, matrices corresponding to unitary operators are necessarily symplectic.

The inverse of a symplectic matrix $\mathbf{S}$ can be verified to be $\mathbf{J}\mathbf{S}^\top\mathbf{J}^\top$, which can also be seen to be symplectic through direct calculation. It is a straightforward exercise to show that the (matrix) product of two symplectic matrices is likewise symplectic. As $\mathbf{I}$ is trivially symplectic and matrix multiplication associative, the symplectic matrices together with matrix multiplication fulfill the four requirements of a group: closure, existence of an inverse element, associativity of the group operation and existence of an identity element. This group, denoted by $\mathrm{Sp}(2N, \mathbb{R})$, is called the symplectic group and it can be shown that mode transformations induced by quadratic Hamiltonians $H = \mathbf{x}^\top\mathbf{M}\mathbf{x}$ introduced in previous Section can be represented by transformations of the form $\mathbf{y} = \mathbf{S}\mathbf{x}$, where $\mathbf{S} \in \mathrm{Sp}(2N, \mathbb{R})$, allowing for an efficient way to compute such dynamics.

To see what kind of states can be generated with the elements of $\mathrm{Sp}(2N, \mathbb{R})$, it is convenient to consider the covariance matrix

$$\mathrm{cov}(\mathbf{x}) = \frac{1}{2}\langle[\mathbf{x}, \mathbf{x}^\top]_+\rangle - \frac{1}{2}[\langle\mathbf{x}\rangle, \langle\mathbf{x}\rangle^\top]_+. \tag{3.12}$$

If $\mathbf{y} = \mathbf{S}\mathbf{x}$, the corresponding transformation of the covariance matrix is simply

$$\begin{aligned}\mathrm{cov}(\mathbf{y}) = \mathrm{cov}(\mathbf{S}\mathbf{x}) &= \frac{1}{2}\langle[\mathbf{S}\mathbf{x}, \mathbf{S}\mathbf{x}^\top]_+\rangle - \frac{1}{2}[\langle\mathbf{S}\mathbf{x}\rangle, \langle\mathbf{S}\mathbf{x}\rangle^\top]_+ \\ &= \frac{1}{2}\mathbf{S}\langle[\mathbf{x}, \mathbf{x}^\top]_+\rangle\mathbf{S}^\top - \frac{1}{2}\mathbf{S}[\langle\mathbf{x}\rangle, \langle\mathbf{x}\rangle^\top]_+\mathbf{S}^\top \\ &= \mathbf{S}\mathrm{cov}(\mathbf{x})\mathbf{S}^\top.\end{aligned} \tag{3.13}$$

A key state characterized completely by the covariance matrix is the thermal state of temperature T. In the non-interacting basis (3.3), it is diagonal with elements given by the expectation values

$$\langle Q_i^2 \rangle = \left(n_i + \frac{1}{2} \right) \Omega_i^{-1}, \quad \langle P_i^2 \rangle = \left(n_i + \frac{1}{2} \right) \Omega_i, \tag{3.14}$$

where $n_i = (\exp(\Omega_i/T) - 1)^{-1}$ is the thermal expectation value of $a_i^\dagger a_i$. In fact, a theorem due to Williamson [79] implies that any covariance matrix $\mathrm{cov}(\mathbf{x})$ can be decomposed as $\mathbf{S}\boldsymbol{\Delta}_{th}\mathbf{S}^\top$, where $\boldsymbol{\Delta}_{th}$ is a diagonal covariance matrix corresponding to some thermal state. It follows that symplectic transformations of such covariance matrices, induced by quadratic Hamiltonians, can generate all states characterized by the covariance matrix. These states are exactly the Gaussian states, characterized by a Gaussian Wigner function, or equivalently, Gaussian characteristic function. It can be shown that they are the only pure states with a positive Wigner function [80, 81].

To be precise, general bilinear Hamiltonians have additional terms proportional to $a_i^\dagger$ and a_i called linear terms, which are necessary to generate displacement, i.e. transformations of the form $\langle \mathbf{x} \rangle \to \langle \mathbf{x} \rangle + \mathbf{d}$, where $\mathbf{d}$ is a vector of real numbers. The evolution generated with such Hamiltonians also preserves Gaussianity of an initial state and can be treated with the so-called affine symplectic group. It is quite natural to omit these linear terms in the context of quantum networks however, as they cannot be interpreted as links, i.e., as pairs of nodes. If the initial state of a quantum network is a Gaussian state with zero mean, it will remain so due to the absence of linear terms. In the rest of this Thesis, all states will have zero mean unless stated otherwise.

Decompositions exist also for symplectic matrices, and the ones where the constituents remain symplectic are of particular interest as they are amenable to a physical interpretation. In particular, Publication IV makes use of the Bloch-Messiah decomposition, also called Euler decomposition, which can be given as follows. Let $\mathrm{SO}(2N)$ be the special orthogonal group of $2N \times 2N$ matrices, i.e. the group of orthogonal matrices with determinant 1. Then $\mathrm{Sp}(2N, \mathbb{R}) \cap \mathrm{SO}(2N)$ is the corresponding set of matrices that are both sympletic and orthogonal. Such matrices can be interpreted as symplectic basis changes and in optics, they are realized with passive devices, i.e. devices that preserve the total number of quanta. It can be shown [82] that any symplectic matrix $\mathbf{S}$ can be decomposed as

$$\mathbf{S} = \mathbf{O}_1 \begin{pmatrix} \mathbf{\Delta}_{\rm sq} & 0 \\ 0 & \mathbf{\Delta}_{\rm sq}^{-1} \end{pmatrix} \mathbf{O}_2, \tag{3.15}$$

where $\mathbf{O}_1, \mathbf{O}_2 \in {\rm Sp}(2n, \mathbb{R}) \cap {\rm SO}(2N)$ and $\mathbf{\Delta}_{\rm sq}$ is a diagonal matrix with positive elements. The diagonal matrix in Eq. (3.15) is symplectic by construction, and corresponds to squeezing, i.e. it lowers the second moment of observables below that of vacuum. Implementing this matrix requires an active device such as interactions between the optical modes induced by an optical parametric process in nonlinear media.

It should be pointed out that the framework introduced above can be adapted to an arbitrary ordering of operators. Indeed, let $\mathbf{y}$ be a new ordering of operators related to $\mathbf{x}$ through $\mathbf{y} = \mathbf{P}\mathbf{x}$, where $\mathbf{P}$ is a permutation matrix, i.e. an orthogonal binary matrix with unit row and column sums. Then direct calculation shows that the commutation relations of $\mathbf{y}$ induce a new matrix $\mathbf{P}\mathbf{J}\mathbf{P}^\top$ which is also orthogonal and skew-symmetric. Moreover, if matrix $\mathbf{S}$ is symplectic with respect to $\mathbf{J}$ then $\mathbf{P}\mathbf{S}\mathbf{P}^\top$ is symplectic with respect to $\mathbf{P}\mathbf{J}\mathbf{P}^\top$—their respective matrix groups are in fact isomorphic—while covariance matrices are related as ${\rm cov}(\mathbf{y}) = \mathbf{P}{\rm cov}(\mathbf{x})\mathbf{P}^\top$. Both Williamson and Bloch-Messiah decompositions can be adapted in the same manner.

Let now $\mathbf{x}(t) = \mathbf{S}\mathbf{x}(0)$ and let the initial state be Gaussian. Then the evolution of the state is fully characterized by the corresponding transformation on the covariance matrix. In the present case, the symplectic matrix giving the dynamics may be found as follows. By defining the vector of operators (3.3) to be $\mathbf{X}^\top = \{Q_1, ..., Q_N, P_1, ..., P_N\}$, the transformation that diagonalizes the network Hamiltonian can be expressed as

$$\mathbf{X} = \begin{pmatrix} \mathbf{K}^\top & 0 \\ 0 & \mathbf{K}^\top \end{pmatrix} \mathbf{x}; \tag{3.16}$$

a direct calculation shows that this matrix is an element of ${\rm Sp}(2N, \mathbb{R}) \cap {\rm SO}(2N)$.

As the Hamiltonian (3.4) is that of noninteracting oscillators, the equations of motion are simple in terms of $\mathbf{X}$. By defining the auxiliary diagonal matrices with elements $\mathbf{\Delta}^{\Omega}_{\cos\, ii} = \cos(\Omega_i t)$ and $\mathbf{\Delta}^{\Omega}_{\sin\, ii} = \sin(\Omega_i t)$, they can

be expressed as

$$\begin{pmatrix} \mathbf{Q}(t) \\ \mathbf{P}(t) \end{pmatrix} = \begin{pmatrix} \boldsymbol{\Delta}^{\Omega}_{\cos} & \boldsymbol{\Delta}_{\boldsymbol{\Omega}}^{-1}\boldsymbol{\Delta}^{\Omega}_{\sin} \\ -\boldsymbol{\Delta}_{\boldsymbol{\Omega}}\boldsymbol{\Delta}^{\Omega}_{\sin} & \boldsymbol{\Delta}^{\Omega}_{\cos} \end{pmatrix} \begin{pmatrix} \mathbf{Q}(0) \\ \mathbf{P}(0) \end{pmatrix}, \tag{3.17}$$

where the matrix acting on the vectors is, of course, symplectic. In this Thesis, the initial state of the network will be a stationary state of the Hamiltonian (3.1), i.e a thermal state described by the diagonal covariance matrix of $\mathbf{X}(0)$

$$\mathrm{cov}(\mathbf{X}(0)) = \begin{pmatrix} \langle \boldsymbol{\Delta}^2_{\mathbf{Q}} \rangle & 0 \\ 0 & \langle \boldsymbol{\Delta}^2_{\mathbf{P}} \rangle \end{pmatrix}, \tag{3.18}$$

where the elements are given by the expectation values (3.14). It is then convenient to find the symplectic matrix giving $\mathbf{x}(t)$ in terms of $\mathbf{X}(0)$. This can be done with the help of (3.16), and the result is

$$\begin{pmatrix} \mathbf{q}(t) \\ \mathbf{p}(t) \end{pmatrix} = \begin{pmatrix} \mathbf{K}\boldsymbol{\Delta}^{\Omega}_{\cos} & \mathbf{K}\boldsymbol{\Delta}_{\Omega}^{-1}\boldsymbol{\Delta}^{\Omega}_{\sin} \\ -\mathbf{K}\boldsymbol{\Delta}_{\Omega}\boldsymbol{\Delta}^{\Omega}_{\sin} & \mathbf{K}\boldsymbol{\Delta}^{\Omega}_{\cos} \end{pmatrix} \begin{pmatrix} \mathbf{Q}(0) \\ \mathbf{P}(0) \end{pmatrix}. \tag{3.19}$$

Using this symplectic matrix, $\mathrm{cov}(\mathbf{x}(t))$ can be determined from $\mathrm{cov}(\mathbf{X}(0))$ of Eq. (3.18). One could also consider non-stationary initial states for the network, as briefly discussed near the end of Section 2.2 in Publication III.

If they are needed, the corresponding expressions for the dynamics of the quadrature operators can be found using Eqs. (3.5) and (3.7). They are

$$\begin{pmatrix} \mathbf{Q}'(t) \\ \mathbf{P}'(t) \end{pmatrix} = \begin{pmatrix} \boldsymbol{\Delta}^{\Omega}_{\cos} & \boldsymbol{\Delta}^{\Omega}_{\sin} \\ -\boldsymbol{\Delta}^{\Omega}_{\sin} & \boldsymbol{\Delta}^{\Omega}_{\cos} \end{pmatrix} \begin{pmatrix} \mathbf{Q}'(0) \\ \mathbf{P}'(0) \end{pmatrix} \tag{3.20}$$

for the normal modes and

$$\begin{pmatrix} \mathbf{q}'(t) \\ \mathbf{p}'(t) \end{pmatrix} = \begin{pmatrix} \mathbf{K}_1 \boldsymbol{\Delta}_{\cos}^{\Omega} & \mathbf{K}_1 \boldsymbol{\Delta}_{\sin}^{\Omega} \\ -\mathbf{K}_2 \boldsymbol{\Delta}_{\sin}^{\Omega} & \mathbf{K}_2 \boldsymbol{\Delta}_{\cos}^{\Omega} \end{pmatrix} \begin{pmatrix} \mathbf{Q}'(0) \\ \mathbf{P}'(0) \end{pmatrix}, \tag{3.21}$$

for the network oscillators, where matrices $\mathbf{K}_1 = \sqrt{\boldsymbol{\Delta}_\omega}\mathbf{K}\sqrt{\boldsymbol{\Delta}_\Omega^{-1}}$ and $\mathbf{K}_2 = \sqrt{\boldsymbol{\Delta}_\omega^{-1}}\mathbf{K}\sqrt{\boldsymbol{\Delta}_\Omega}$ follow from Eq. (3.7). The initial covariance matrix $\mathrm{cov}(\mathbf{X}'(0))$ is diagonal with elements $\langle Q_i'^2 \rangle = \langle P_i'^2 \rangle = n_i + 1/2$.

It may be asked what is lost by restricting the studies to Gaussian states. Gaussianity implies that the dynamics can always be efficiently simulated on a classical computer, while this is not in general true for non-Gaussian states [83]. In particular, this means that non-Gaussianity is necessary to have dynamics that is hard or intractable to simulate with classical means, providing strong motivation to emulate it with experimentally controlled quantum systems. A possible approach would be to first implement Gaussian dynamics of the network Hamiltonian and then try to introduce additional operations suitable to a multimode scenario to de-Gaussify the state. The first step is introduced in Chapter 7, while the second is still missing. Possible operations needed for it include mode-selective single photon subtraction, which has recently been experimentally implemented as reported in [84]. This allows the subtraction of a single photon from any given mode or a superposition of modes, leading to a non-Gaussian multimode state. The properties of such states, including ones where mode-selective single photon addition has been performed, have been theoretically investigated [85] and found to have, e.g., entanglement properties specific to non-Gaussian states. Both operations can potentially lead to dynamics that cannot be simulated efficiently [86].

3.4 Open quantum systems theory

A quantum system not interacting with other systems is said to be closed, while in the other case the system is said to be open. All realistic quantum systems interact with their surroundings, which makes them open. A somewhat more precise definition is to take closed systems to be the quantum systems undergoing unitary evolution given by a (possibly time-dependent) Hamiltonian. In contrast, the evolution of an open quantum system is induced by the unitary evolution of the closed total system including the

environment and interaction terms, and as such is described in terms of so-called dynamical maps, which in a sense generalize the notion of unitary evolution of closed systems. While a dynamical map Λ_t can always be formally given using a trace over the environment degrees of freedom on the total unitary evolution, one of the goals of open quantum systems theory is to find descriptions of open system dynamics in terms of a restricted set of relevant variables, such as an equation of motion for the open system density matrix (quantum master equation) or degrees of freedom (Heisenberg equation). It is often applied in situations where finding the Hamiltonian dynamics of the full system is either impractical or impossible.

The dynamics of open quantum systems have features that are not present in unitary evolution, such as dissipation, i.e. irreversible loss of excitations or information to the environment. While contact with a finite environment may not lead to truly irreversible dynamics, in many practical situations finite-size effects can be ignored. In the Rubin model [87], the environment is a semi-infinite chain of identical harmonic oscillators interacting with springlike interaction terms of constant magnitude. This corresponds to a particular choice for matrix $\mathbf{L}$ for the network Hamiltonian (3.1), i.e. that of a semi-infinite path graph with constant weights. The diagonal form (3.4) of a (chain or generic) quantum network is more akin to the environment of the Caldeira-Legget model [88] instead. In this model, a particle with a mass m_S, position operator q_S and potential $V(q_S)$ is coupled to infinitely many harmonic oscillators, not interacting with each other, with a linear interaction term. The full Hamiltonian is

$$H = \frac{p^2}{2m_S} + V(q_S) + \sum_i \left(\frac{p_i^2}{2m_i} + \frac{1}{2} m_i \omega_i^2 q_i^2 \right) - \sum_i g_i q_S q_i, \tag{3.22}$$

where m_i, p_i, q_i and ω_i are the mass, position, momentum and frequency of the environment oscillator i, respectively, and g_i is the interaction strength between it and the open system.

The interaction with the environment leads to dissipation as well as renormalization of $V(q_S)$. The latter effect may be eliminated by introducing a counter-term in the above Hamiltonian. Due to the harmonic potential of the environment oscillators and linearity of the interaction term, it is possible to derive exact Heisenberg equations of motion for the system variables where the dynamics of the environment variables has been elim-

inated[3]. In such equations of motion, it is convenient to introduce a term $\gamma(t)$ called the damping kernel or memory-friction kernel, accounting for time dependent dissipation and memory effects. Let the interaction begin at $t = 0$. Then $\gamma(t)$ is defined to vanish for times $t < 0$, while otherwise it is of the form

$$\gamma(t) = \frac{1}{m_S} \sum_i \frac{g_i^2}{m_i \omega_i^2} \cos(\omega_i t). \tag{3.23}$$

A closely related quantity in the frequency domain, denoted by $J(\omega)$, is called the spectral density of environmental couplings, or simply spectral density. It characterizes completely the relevant information in both H_E and H_I, and reads

$$J(\omega) = \frac{\pi}{2} \sum_i \frac{g_i^2}{m_i \omega_i} \delta(\omega - \omega_i), \tag{3.24}$$

where δ is the Dirac delta function. In the limit where the frequencies ω_i form a continuum, $J(\omega)$ becomes a continuous function of frequency, and the relation between it and $\gamma(t)$ may be expressed as

$$\begin{aligned} J(\omega) &= m_S \omega \int_0^\infty \gamma(t) \cos(\omega t) \mathrm{d}t, \\ \gamma(t) &= \frac{1}{m_S} \frac{2}{\pi} \int_0^\infty \frac{J(\omega)}{\omega} \cos(\omega t) \mathrm{d}\omega. \end{aligned} \tag{3.25}$$

Both quantities are used to study quantum networks as environments in the next Chapter.

In practice, phenomenological spectral densities based on physically motivated assumptions and experimental data are often used. Power-law spectral densities proportional to ω^l for some positive real number l are a typical example. To avoid divergence of certain physical quantities depending on $J(\omega)$, a high-frequency cutoff is often introduced so that $J(\omega)$ vanishes at the limit $\omega \longrightarrow \infty$. In these cases, the power-law holds up to a characteristic upper limit of frequency. These spectral densities are called Ohmic,

[3] See, e.g., Section 3.6.3 in [75]

sub-Ohmic and super-Ohmic for $l = 1$, $0 < l < 1$ and $l > 1$, respectively, where the name Ohmic originates from a correspondence with a series resistor in an electrical circuit. While most $J(\omega)$ considered later will be much more structured, an Ohmic spectral density with an exponential cut-off $\exp(-\omega/\omega_c)$ controlled by parameter ω_c is considered in Publication II.

Although master equations for the open system density matrix $\rho(t)$ are not used in this Thesis, they are closely related to the non-Markovianity of the open system dynamics, an aspect considered particularly in Publications II and III. In short, non-Markovianity refers to deviations from memoryless dynamics conforming to the Markov approximation, where it is assumed that the correlation time scale of the environment is so short compared to the rate of system state change due to dissipation that the environment rapidly forgets any information leaked from the open system, making the dynamics memoryless. Markovianity can also be defined as divisibility of the dynamical map Λ_t, i.e. the property that it may be decomposed as $\Lambda_t = V_{ts}\Lambda_s$ where $t > s > 0$ and the so-called propagator V_{ts} is a positive map that will remain positive when tensored with an identity map acting on a Hilbert space of dimension d for all dimensions d, i.e. a completely positive map. Non-Markovianity can result from, e.g., strong interactions, an enviroment with a complicated $J(\omega)$, and a finite environment. Aside from being of fundamental interest, non-Markovianity can sometimes be useful, for instance by leading to revivals of previously lost quantum resources in the state of an open quantum system.

Generally speaking, non-Markovianity is a multifaceted phenomenon. For instance, time-local master equations, where $\frac{\mathrm{d}}{\mathrm{d}t}\rho(t)$ explicitly depends only on $\rho(t)$, have been traditionally called Markovian master equations, while those with a memory kernel accounting for terms of the form $\rho(s)$ where $s < t$, i.e., depending on the previous history of the system state evolution, have been thought to correspond to non-Markovian dynamics. This simple view is problematic. For instance, memory kernel master equations can be recast in time-local form and vice versa [89]. Furthermore, time-local master equations can, in fact, be used to describe dynamics where memory effects are present [90]. To address this problem, many witnesses and measures of non-Markovianity have been proposed, as explained in many excellent review articels such as [91, 92]. In Section 4.3 this Thesis focuses on a measure and witness suitable for continuous variable systems, based on tracking the evolution of a metrological quantity depending on discord-type correlations in a bipartite open system. The non-monotonicity of this

evolution witnesses the non-divisibility of the dynamical map.

As a closing remark, it should be mentioned that while in the Publications introduced in this Thesis the network is taken to be a finite environment for an open quantum system, a complementary viewpoint of open quantum networks immersed in a heat bath can be considered to study, e.g., decoherence in quantum information processors modeled by quantum networks [93, 94], or dissipation induced collective dynamics in quantum networks, such as synchronization [30] or superradiance [95].

Chapter 4

Quantum networks as environments

This Chapter introduces results from Publications I-III on quantum networks as tunable environments for an open quantum system. Throughout this Chapter, the state of the network is assumed to be the stationary state of Hamiltonian (3.1), corresponding to the thermal covariance matrix (3.18). Furthermore, the initial state of the total system, i.e., open quantum system (probe) plus environment (quantum network), is assumed to be factorized.

4.1 Network spectral density

Consider a quantum harmonic oscillator with the Hamiltonian $H_S = (p_S^2 + \omega_S^2 q_S^2)/2$, coupled to a quantum network with an interaction Hamiltonian $H_I = -\sum_i^N k_i q_S q_i$, and let $\mathbf{k}^\top = \{k_1, k_2, \dots\}$ be the vector of coupling strengths between the position operators. With the network Hamiltonian H_E given by Eq. (3.1), the full Hamiltonian $H = H_S + H_E + H_I$ may be expressed as

$$H = \frac{p_S^2}{2} + \frac{\omega_S^2 q_S^2}{2} + \frac{\mathbf{p}^\top \mathbf{p}}{2} + \mathbf{q}^\top \mathbf{A} \mathbf{q} - q_S \mathbf{k}^\top \mathbf{q}. \tag{4.1}$$

In terms of the operators (3.3) of the non-interacting modes, H_E is given by Eq. (3.4) while H_I becomes

$$H_I = -q_S \mathbf{k}^\top \mathbf{q} = -q_S \mathbf{k}^\top \mathbf{K}\mathbf{Q} = -q_S \mathbf{g}^\top \mathbf{Q}, \tag{4.2}$$

where the last equality follows from the introduction of $\mathbf{g} = \mathbf{K}^\top \mathbf{k}$ with elements $\mathbf{g}_i = g_i$, i.e. the interaction strengths between q_S and each Q_i. Together with the diagonal Hamiltonian (3.4), the full Hamiltonian is

$$H = \frac{p_S^2}{2} + \frac{\omega_S^2 q_S^2}{2} + \sum_i^N \left(\frac{P_i^2}{2} + \frac{\Omega_i^2 Q_i^2}{2} \right) - \sum_i^N g_i q_S Q_i, \tag{4.3}$$

a special case of the Hamiltonian (3.22). The network can be interpreted as an environment for the open system with Hamiltonian H_S. Whenever the initial state of the full system is Gaussian, the exact dynamics can be determined along the lines of Eqs. (3.17) and (3.19), as shown in detail in, e.g., Section 3.1 of Publication III. The extension to multiple external oscillators is straightforward, and considered briefly in Chapter 6.

With the full Hamiltonian in this form, one can now define both the damping kernel (3.23) and the spectral density (3.24) associated with the network. This is achieved by simple replacements $m_i, m_S \to 1$ and $\omega_i \to \Omega_i$. Both $\gamma(t)$ and $J(\omega)$ can be used to characterize a given network as an environment.

The predominant difference with typical phenomenological spectral densities like the ones described in Section 3.4, is that for finite networks considered here, $J(\omega)$ is discrete. On the other hand, $\gamma(t)$ remains continuous. To better understand how the network is like from the point of view of the open system and to allow comparisons with continuous spectral densities, one may define the spectral density with the help of relation (3.25) as

$$J(\omega) = \omega \int_0^{t_{\max}} \gamma(t) \cos(\omega t) \mathrm{d}t, \tag{4.4}$$

where the upper limit of infinity has been replaced by a finite interaction time $t_{\max} > 0$. Strictly speaking, this defines a new function $J(\omega, t_{\max})$, but for reasons that will become clear in a moment, such distinction is not made in the attached Publications.

Quantum networks can be roughly divided in two categories: those

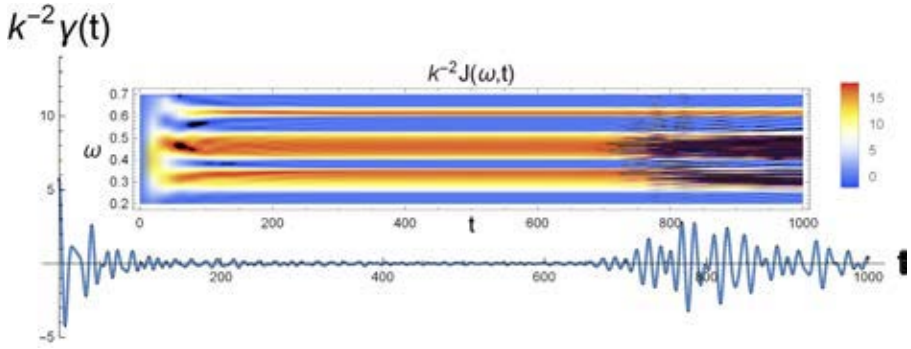

Figure 4.1: The damping kernel $\gamma(t)$ of a periodic chain as a function of interaction time t, when system is coupled to the first oscillator with coupling strength k. Inset: the corresponding spectral density $J(\omega, t)$ with three bands. Notice that the horizontal axes are identical. The chain has $N = 60$ nodes where coupling strengths are $c_1 = 0.1$ except for every third coupling strength, which is $c_2 = 0.06$. The effective frequencies $\tilde{\boldsymbol{\omega}}$ are similarly periodic, with values $\tilde{\omega}_1 = \sqrt{0.45}$ and $\tilde{\omega}_2 = \sqrt{0.41}$.

where the spectral density assumes a continuous and fixed form for a transient in interaction times, the duration of which depends on the structure and size of the network, and those where this does not occur. This can be observed in the damping kernel: for the former, for t in the transient, $\gamma(t) \sim 0$. Networks with symmetries seem to tend to fall into the former class while more complex networks often fall in the latter.

This is exemplified in Fig. 4.1, where the damping kernel of a periodic chain is shown. The chain has periodic couplings with every third coupling strength weaker, and the frequencies of the first and last oscillators are increased to achieve the same periodicity in the effective frequencies. The inset shows the spectral density with three bands (red) with the non-resonant frequencies denoted by blue. It quickly assumes a static form, which is eventually lost due to finite size effects, seen in $\gamma(t)$ as revivals of oscillations, and at the limit $t \longrightarrow \infty$ the spectral density becomes fully discrete according to Eq. (3.24). At variance, for networks without translational symmetry the discrete spectrum tends to emerge quickly. This makes sense, as same lattices of different sizes can be expected to be effectively the same environment in the continuum regime of interaction times, but this is

not true for generic complex networks as they are in general not self-similar enough. A comparison between a symmetric and random network can be found in Figure 1 of Publication III.

A possible supplementary approach, discussed at the end of Section 3.1 in Publication III, is to consider the Gaussian quantum channel induced by the contact with the network. The action of the channel on the open system covariance matrix is of the form $\mathrm{cov}(\{q_S(t), p_S(t)\}^\top) = \mathbf{C}(t)\mathrm{cov}(\{q_S(0), p_S(0)\}^\top)\mathbf{C}^\top(t) + \mathbf{L}(t)$, where $\mathbf{C}(t)$ and $\mathbf{L}(t)$ are real matrices and $\mathbf{L}(t)$ is symmetric. These matrices are easily found once the symplectic matrix induced by the total Hamiltonian is at hand.

4.2 Engineering of spectral density

As noted in Section 3.3, the spectral density captures completely the relevant information in H_E and H_I for full Hamiltonians of the form (3.22). They remain a central object also for finite environments such as quantum networks. Publication I considers not only what kind of spectral densities networks have, but the complementary perspective of how the spectral density changes with the network structure.

The starting point used in Publication I is a homogeneous chain of length N, i.e. a chain where effective frequencies and coupling strengths are both uniform. Then the Hamiltonian (3.1) is simplest to express in terms of the unweighted adjacency matrix $\mathbf{V}$ of a path graph as

$$H_E = \frac{\mathbf{p}^\top \mathbf{p}}{2} + \frac{\mathbf{q}^\top(\omega_0^2 \mathbf{I} + g(2\mathbf{I} - \mathbf{V}))\mathbf{q}}{2}, \tag{4.5}$$

where ω_0 controls the oscillator frequencies and g is the uniform coupling strength. This corresponds to bare frequencies that coincide with ω_0 for the oscillators other than first and last, which have a higher bare frequency. A finite Rubin chain is recovered with the choice $\omega_0 = 0$. The matrix $\mathbf{K}$ taking the Hamiltonian to diagonal form is independent of ω_0, but the eigenfrequencies change. The smallest eigenfrequency coincides with ω_0 while the difference between the smallest and largest decreases as ω_0 is increased.

Suppose the open system is coupled to one of the end nodes. As noted in Publication I, the corresponding $J(\omega)$ has a single band. As shown in

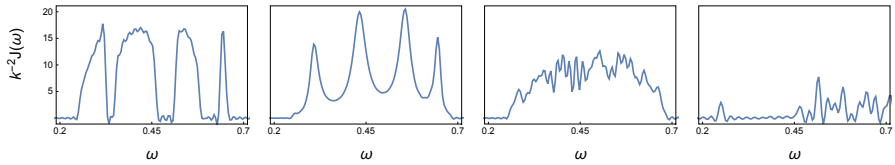

Figure 4.2: Examples of engineered spectral densities. From the left, the first three are based on a chain with Hamiltonian (4.5) with $N = 200$, $g = 0.1$ and $\omega_0 = 0.25$ while the last example is an ER random network with same parameters. Notice that the vertical axes are identical in all panels. Refer to main text for details.

the first example in Fig. 4.2, adding periodicity to the coupling strengths splits the $J(\omega)$ into multiple bands, controlled by the period: with every n-th coupling weaker, there will be n bands. Increasing the difference in coupling strengths widens the band gaps. In this particular case, four bands are present.

Instead of tuning the coupling strengths, a similar effect can be achieved by adding just one additional link as a shortcut near the beginning of the chain. While this does not create true band gaps, $J(\omega)$ will have spikes, with a number controlled by how many nodes are between the shortcut and the open system. This is shown in the second example of Fig. 4.2, where the additional link is between nodes 5 and 150. It might seem suprising that the addition of just one more link can have a significant effect on the shape of $J(\omega)$. In fact, it is the change in matrix $\mathbf{K}$ that is mostly responsible.

The next example has been made by adding to the chain 30 randomly chosen links with a weak coupling strength $0.06g$. This leads to a complicated fine structure added to the band. The final example is an ER random network, which tend to have complicated spectral densities that can change completely when coupling to different nodes in the network.

If generic interaction is considered where $\mathbf{k}$ is not restricted, a very rich variety of $J(\omega)$ becomes possible even for a fixed network, as each possible choice results in different coupling strengths $\mathbf{g}$ to modes $\mathbf{Q}$ through $\mathbf{g} = \mathbf{K}^\top \mathbf{k}$. In Publication I, this was not fully explored, but coupling the open system to nodes of several networks was briefly considered. In this case, the spectral densities of each network are simply added up, weighted according to interaction strengths to each of them. Generally speaking, ad-

ditional links between the system and a single network can either increase or decrease the magnitude of the elements of $\mathbf{g}$ since the elements of $\mathbf{K}$ can have different signs. In particular, a judicious choice of $\mathbf{k}$ can even disconnect the system from an eigenmode. The effect of generic $\mathbf{k}$ on transport is briefly considered in Chapter 6. It is well-known that if the oscillator frequencies and coupling strengths can be freely tuned instead, any given spectral density can be realized with just a chain.

Realization of given spectral density

Let the number of nodes N be fixed to some finite value, and consider a given continuous $J(\omega)$. Finding $\mathbf{g}$ and $\mathbf{\Omega}$ such that Eq. (4.4) coincides with $J(\omega)$ to a good approximation for a transient can sometimes be convenient, as this allows one to study the exact dynamics of a finite system that, in the continuum regime, can emulate an infinite bath of oscillators. One should choose the N frequencies $\mathbf{\Omega}$ first; they should cover the non-vanishing parts of the given spectral density. Then the values of $\mathbf{g}$ needed to realize $J(\omega)$ can be readily found from the values of the spectral density at the chosen frequencies, as recalled at the end of Section 3.2 in Publication III. The resulting total system now corresponds to a Hamiltonian of the form (4.3). Additonally, once both $\mathbf{g}$ and $\mathbf{\Omega}$ are at hand, a simple way to find the corresponding chain of oscillators is to add an extra row and a column to the diagonal matrix $\Delta_{\mathbf{\Omega}}$ to account for $\mathbf{g}$ and the open system frequency and tridiagonalizing the resulting real symmetric $(N+1)\times(N+1)$ matrix with a Householder transformation [96]. The resulting tridiagonal matrix corresponds to a system coupled to one of the ends of a chain of oscillators with nearest neighbor couplings, with a total Hamiltonian of the form (4.1).

As noted just previously, a network can have as many spectral densities as there are admissible choices for $\mathbf{k}$, but they are all restricted ultimately by matrix $\mathbf{K}$. An interesting problem is then to consider how to realize two or more given $J(\omega)$ with a single connected network. If disconnected networks are allowed, the problem becomes trivial: any set of spectral densities can always be realized, with a different connected component assigned for each.

Starting from the eigenfrequencies, in principle one could consider the $J(\omega)$ with the widest spectrum and ensure it falls within $\mathbf{\Omega}$. Next, it should be checked if the corresponding coupling strengths are all of the form $\mathbf{K}^\top\mathbf{k}$ for some admissible $\mathbf{k}$.

If $\mathbf{k}$ is allowed to have any real elements, the problem becomes trivial:

for each $\mathbf{g}$, one should simply use $\mathbf{Kg}$. Then, in principle, any set of spectral densities may be realized but each will have the same discrete set of eigenfrequencies; for most, many elements in $\mathbf{g}$ might be vanishing to allow the spectral densities to effectively have different resonant frequencies. It might be, however, quite reasonable to restrict $\mathbf{k}$ further. This restricted case might warrant further attention in future studies.

4.3 Network non-Markovianity

Non-Markovianity of the model is studied in Publications II and III. In both cases, it is quantified using a measure and a witness based on the non-monotonic evolution of the Gaussian interferometric power under non-divisible dynamical maps [97].

Gaussian interferometric power $\mathcal{G}$ quantifies the worst-case precision achievable in a black-box phase estimation using a bipartite Gaussian probe with modes A and B. By subjecting one of the modes of the probe to the Gaussian channel, the unknown phase leaves a fingerprint in the state; how well the phase can subsequently be estimated is completely determined by the initial state of the probe. In this scenario, $\mathcal{G}$ can be determined directly from the symplectic invariants of the two-mode covariance matrix $\boldsymbol{\sigma}_{AB}$. As it vanishes for product states, it is a measure of non-classical correlations between the modes.

Let the initial covariance matrix $\boldsymbol{\sigma}_{AB}$ be fixed. For divisible channels, $\mathcal{G}(\boldsymbol{\sigma}_{AB})$ is monotonically non-increasing, meaning that $\frac{\mathrm{d}}{\mathrm{d}t}\mathcal{G}(\boldsymbol{\sigma}_{AB}) \leq 0$. Let $\mathcal{D}(t) = \frac{\mathrm{d}}{\mathrm{d}t}\mathcal{G}(\boldsymbol{\sigma}_{AB})$. Now the non-Markovianity of the probe dynamics with the initial covariance matrix $\boldsymbol{\sigma}_{AB}$, and up to interaction time $t_{\max} > 0$, may be quantified by

$$\mathcal{N}_{\mathrm{GIP}} = \int_0^{t_{\max}} \left(|\mathcal{D}(t)| + \mathcal{D}(t)\right) \mathrm{d}t. \tag{4.6}$$

While the original definition involves a maximization over the initial states and considers the non-Markovianity over the entire evolution, it is currently an open question how the maximization should be carried out, while the finite upper limit is considered here due to the finite size of the environment. Indeed, as the goal is to assess non-Markovianity arising from other sources than finite-size effects, $t_{\max}$ will be taken to be small enough

to avoid them. Since strong numerical evidence suggests that squeezed thermal states can optimize $\mathcal{N}_{\mathrm{GIP}}$ [97], the initial state is fixed to such a state, with a covariance matrix of the form

$$\boldsymbol{\sigma}_{AB}^{STS} = (n_{th} + \tfrac{1}{2}) \begin{pmatrix} \mathbf{\Delta_x} & \mathbf{\Delta_y} \\ \mathbf{\Delta_y} & \mathbf{\Delta_x} \end{pmatrix}, \tag{4.7}$$

where $\mathbf{x}^\top = \{\cosh(2r), \cosh(2r)\}$, $\mathbf{y}^\top = \{\sinh(2r), -\sinh(2r)\}$, r is the squeezing parameter and n_{th} is the mean number of thermal excitations.

Publication II focuses on Hamiltonians of the form (4.3) corresponding to a fixed Ohmic spectral density $J(\omega) = \lambda\omega \exp(-\omega/\Omega)$, where parameter λ controls the overall interaction strength and parameter Ω the cutoff. The studies are carried out using the exact dynamics of a finite system mimicking an infinite heat bath, as well as analytically in the weak coupling approximation with full counting statistics formalism. The two quantities of interest are $\mathcal{N}_{\mathrm{GIP}}$ and the excitation backflow, introduced in [98], which is quantified in Publication II with

$$\langle \Delta q \rangle_{\mathrm{back}} = \frac{1}{2} \int_0^{t_{\max}} (|\theta(t)| + \theta(t)) \mathrm{d}t, \tag{4.8}$$

where $\theta(t)$ is the excitation flow per unit of time. This quantity measures the non-monotonicity of the evolution of system excitations.

While $\langle \Delta q \rangle_{\mathrm{back}}$ is known to behave in a similar way to backflow of information in the case of qubits [98], it is found that for continuous variable systems, above a certain threshold of interaction strength, only very weakly dependent on the environment temperature, $\langle \Delta q \rangle_{\mathrm{back}}$ vanishes while the dynamics is still non-Markovian according to $\mathcal{N}_{\mathrm{GIP}}$. To better understand the cause, the total change in energy in the system, environment and interaction terms was investigated in both weak and strong interaction strengths. It was found that in the case of weak interaction, the system receives a small amount of energy from the environment and all of the energy from the interaction term, while in the opposite case energy from the interaction term flows to both the system and the environment, causing $\langle \Delta q \rangle_{\mathrm{back}}$ to vanish.

In Publication III, the studies are extended to complex networks derived

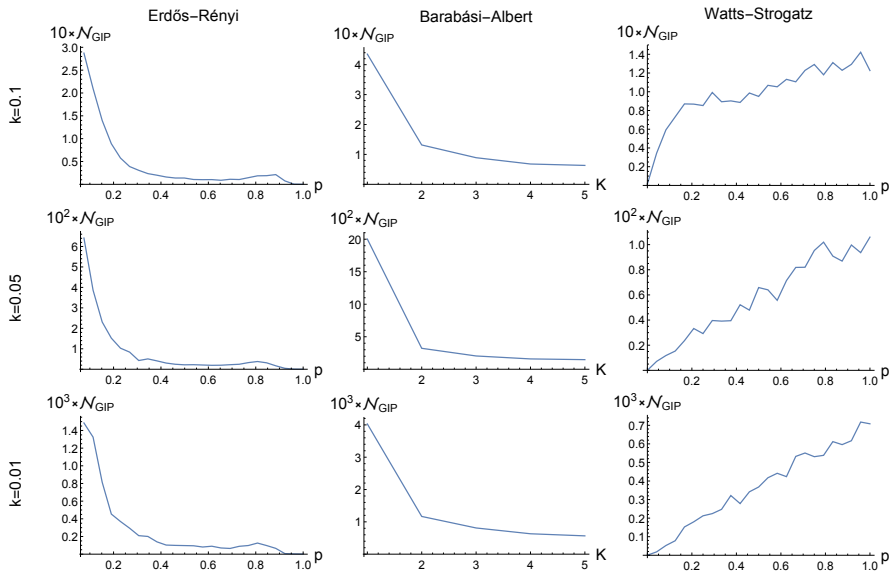

Figure 4.3: Non-Markovianity of complex networks. The columns correspond to the type and the rows to interaction strength between the network and the system. Network size is fixed to N = 30 while a parameter controlling the structure is varied. Links increase with the parameter for ER and BA networks, which suppresses non-Markovianity. For WS networks the number of links is constant but p controls the likelihood of a link being randomly rewired; $p = 0$ corresponds to a circular lattice while $p = 1$ rewires all links. Non-Markovianity is seen to increase with the rewirings. Results are averaged over 1000 realizations for each parameter value. This Figure has been reproduced from Publication III.

from ER, BA and WS random graph models and the effect of varying the network parameters on $\mathcal{N}_{\mathrm{GIP}}$ is studied for weak, intermediate and strong coupling strengths k between the open system and network, while the open system is set to be resonant with an eigenfrequency in the network. The network Hamiltonians are of the form (3.1) with the coupling strengths and bare frequencies have uniform values $g = 0.1$ and $\omega_0 = 0.2$, respectively, while the size is fixed to $N = 30$ nodes. The initial two-mode covariance matrix $\boldsymbol{\sigma}_{AB}^{STS}$ has parameters set to $r = \frac{1}{2}\cosh^{-1}(5/2)$ and $n_{th} = \frac{1}{2}$ while the initial state of the network is vacuum. The results are shown in Fig. 4.3.

Increasing the link probability p of ER networks or the connectivity parameter K of BA networks increases the total number of links in the network. The results show that this quickly suppresses the non-Markovianity. Unlike ER and BA networks, WS networks are lattices for a specific parameter value, namely when the rewiring probability $p = 0$. This is seen to lead to Markovian dynamics. As the links are rewired, $\mathcal{N}_{\mathrm{GIP}}$ steadily increases. This indicates that while disorder is necessary for non-Markovianity, with enough links the dynamics can still be almost Markovian even for complex networks.

Chapter 5

Probing of quantum networks

This Chapter introduces results from Publications I and V related to probing of quantum networks. Complementing the previous Chapter where networks were considered as environments for an open quantum system, here it is asked what one can say about a network by knowing or measuring the open system dynamics. While just the possibility to tune the open system frequency can reveal much, in principle full knowledge of the network properties requires the ability to sequentially couple the open system to any single and pairs of nodes in the network. The requirement of having to couple to pairs of nodes has implications to the network discrimination problem, introduced and discussed in the final Section.

In our work the state of the network is fixed while matrix $\mathbf{A}$ characterizing the network is assumed to be unknown. Others have considered, e.g., probing an unknown state of a network [49] or assumed that the unweighted adjacency matrix $\mathbf{V}$ is known and investigated the probing of the weights [48]. Still others have considered the use of optimal quantum estimation theory in the context of probing structured reservoirs characterized by an Ohmic spectral density and temperature and studied the estimation of reservoir parameters using either continuous variable [99] or qubit probes [100, 101] to find the conditions on initial probe state, reservoir parameters and interaction time that maximize information gained from measurements on the probe, quantified by quantum Fisher information. Here probing is not considered from this point of view.

5.1 Minimal access probing

Consider a composite system with full Hamiltonian (4.1), and assume that the interaction Hamiltonian H_I is fixed. This fixes the set of coupling strengths $\mathbf{g}$, while the eigenfrequencies $\mathbf{\Omega}$ are uniquely determined by the matrix $\mathbf{A}$ of the network Hamiltonian. In turn, the network spectral density $J(\omega)$ is now fixed according to Eq. (3.24). When the probe is restricted to be coupled to a single given node, the scenario will be referred to as *minimal access probing*. It is clear from $\mathbf{g} = \mathbf{K}^\top \mathbf{k}$ that $\mathbf{g}$ is then directly proportional to a row of $\mathbf{K}$.

Let the state of the network be a thermal state of temperature T. If no assumptions about $\mathbf{A}$ are made, then the quantities that one can hope to gain information of are $J(\omega)$ and the parameters of H_E appearing in it, namely the elements of $\mathbf{g}$ and $\mathbf{\Omega}$, as the effect of the network on the open system dynamics is determined by them. In Publication I, it is checked that when the interaction between the open system and network is weak, the expectation value of the system number operator $\langle n(t)\rangle = \langle a^\dagger(t)a(t)\rangle$ is well-approximated by the analytical expression [102]

$$\langle n(t)\rangle = e^{-J(\omega_S)/\omega_S}\langle n(0)\rangle + (1 - e^{-J(\omega_S)/\omega_S})n_{th}(\omega_S), \tag{5.1}$$

where ω_S is the system frequency and $n_{th}(\omega_S) = (e^{\frac{\omega_S}{T}} - 1)^{-1}$ is the mean number of thermal excitations at system frequency. Consequently, for weak interaction the value of spectral density at system frequency is well-approximated by

$$J(\omega_S) = \frac{\omega_S}{t} \ln\left(\frac{\Delta n(0)}{\Delta n(t)}\right), \tag{5.2}$$

where $\Delta n(t) = n_{th}(\omega_S) - \langle n(t)\rangle$. While it can be seen that the initial state of the probe should be such that $\langle n(t)\rangle \neq n_{th}(\omega_S)$, no other assumptions were made in Publications I and V where Gaussian states for the probe were used throughout; the particular choice of initial state was not found to have a noticable effect on any of the results. The protocol to probe the spectral density is summarized below.

1. Fix $\Delta n(0)$ by initializing the states of the probe and the network.

2. Switch on the interaction Hamiltonian H_I for a time t.
3. Determine $\Delta n(t)$ by measuring $\langle n(t) \rangle$.
4. Determine $J(\omega_S)$ from Eq. (5.2).
5. Repeat steps 1–4 for different values of ω_S to sample the spectral density.

For a concrete example, consider the probing of the periodic chain from Fig. 4.1. Figure 5.1 depicts the spectral densities determined from Eq. (4.4) (solid line) against the values determined from Eq. (5.2) for different values of ω_S (circles). The arrows mark different choices of interaction times t. The continuum regime of this network is shown in a transient where both the calculated and probed values of the spectral density form a continuous, smooth function of the frequency. Eventually the finite size effects manifest, and both quantities begin to approach the form given by Eq. (3.24). Such a transient is typically either very short or not evident at all for more complex networks, as seen, e.g., in Publication IV introduced in Chapter 7 of this Thesis, where probing of $J(\omega)$ of networks generated with the ER, BA and WS random graph models presented in Section 2.2 is used in a simulation of the experimental implementation of these networks.

The eigenfrequencies $\mathbf{\Omega}$ emerge in the discrete regime of dynamics and can be probed similarly to $J(\omega)$. The difference in the behaviour of $\langle n(t) \rangle$ between the eigenfrequencies and the off-resonant frequencies, as observed in Figure 5.2, enables their probing. Initially, one might use a stronger coupling to determine what is the range of frequencies where $\mathbf{\Omega}$ can be found, and then switch to a weak coupling to effectively tell them apart[1]. For certain networks with, e.g., special symmetries, it can happen that $\mathbf{\Omega}$ is approximately or even exactly degenerate, or $\mathbf{g}$ might contain vanishing elements. In the former case the degenerate eigenfrequencies cannot be resolved while in the latter case, lack of interaction makes probing of the corresponding eigenfrequencies impossible. Graph theoretic arguments may be used to show that this is not the case for generic networks.

Once $\mathbf{\Omega}$ is known, the squares of the elements of $\mathbf{g}$ can be determined from the probed values of the spectral density as follows. From the definition of $J(\omega)$ it follows that $\int_0^\infty \frac{2}{\pi} J(\omega) \omega \mathrm{d}\omega = \sum g_i^2$. Writing the integral as

[1]It is reasonable to assume here that N is known, as otherwise it is not in general possible to tell when all eigenfrequencies have been found.

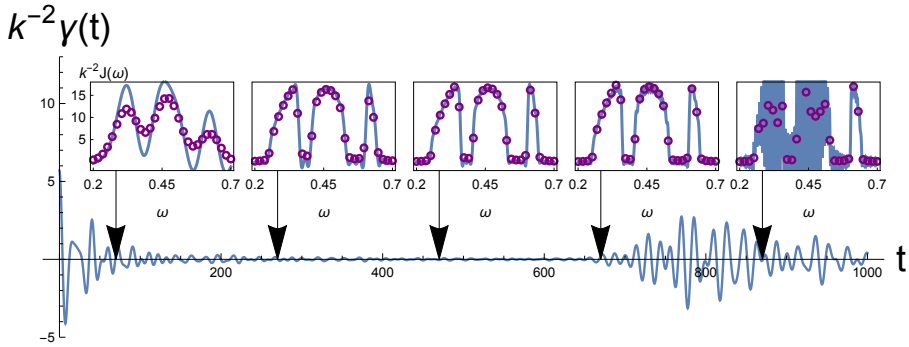

Figure 5.1: Effect of varying the interaction time t in the probing of $J(\omega)$ of the periodic network from Fig. 4.1. In the continuum regime, where $\gamma(t) \sim 0$, $J(\omega)$ calculated with Eq. (4.4) (solid line) and probed with Eq. (5.2) (circles) assume stationary values. Both eventually begin to approach the discrete spectral density of Eq. (3.24). The system and network are initially in a vacuum state and thermal state with $T = 1$, respectively, while the coupling strength $k = 0.01$. All other parameters are as in Fig. 4.1.

a Riemann sum over values $J(\Omega_i)$ and identifying terms in the summations leads to

$$g_i^2 = \frac{2J(\Omega_i)\Omega_i \Delta\Omega_i}{\pi}, \tag{5.3}$$

where the term $\Delta\Omega_i = \Omega_i - \Omega_{i+1}$ comes from the Riemann sum, assuming that $\mathbf{\Omega}$ has been ordered non-increasing. If $\mathbf{k}$ is known, as is reasonable to assume, $\mathbf{g}$ reveals information about matrix $\mathbf{K}$; specifically, with minimal access, one can obtain the squares of the elements of a single row. Signs of these elements are not revealed, which has implications discussed further in the following two Sections.

Because of the underlying graph structure, the eigenfrequencies $\mathbf{\Omega}$ may potentially contain significantly more information about the structure of the network. In particular, a large volume of potentially useful results exists in the field of spectral graph theory, a branch of mathematics concerned with the interplay between graph matrix representations and their spectrum. In Publication V, a special case of identical oscillators and uniform couplings

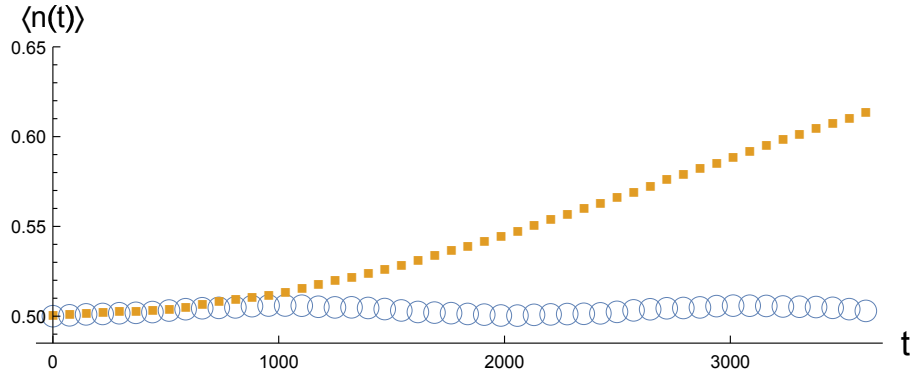

Figure 5.2: Evolution of mean excitations for a probe system weakly coupled to a single node in a network of 40 nodes and 80 randomly chosen links with bare frequency $\omega_0 = 0.2$ and a constant coupling strength $g = 0.1$, with probe frequency coinciding with an eigenfrequency of the network (squares) and just a little above 1% off (circles). The initial state of the probe and the chain were vacuum and thermal state with $T = 0.3$, respectively, while coupling strength between the probe and the chain was $k = 0.0025$. The difference in the dynamics for longer interaction times makes the detection of eigenfrequencies possible. This Figure has been reproduced from Publication V.

is considered. With these assumptions, the Hamiltonian (3.1) may be given as

$$H_E = \frac{\mathbf{p}^\top \mathbf{p}}{2} + \frac{\mathbf{q}^\top (\omega_0^2 \mathbf{I} + g\mathbf{L})\mathbf{q}}{2}, \tag{5.4}$$

where ω_0 is the identical bare frequency of the oscillators, g the constant coupling strength between them, and $\mathbf{L}$ the unweighted Laplace matrix. Let λ_i be the i-th eigenvalue of $\mathbf{L}$. Now

$$\lambda_i = \frac{\Omega_i^2 - \omega_0^2}{g}, \tag{5.5}$$

meaning that when g is known, probing the eigenfrequencies reveals the

Laplace eigenvalues.

The main result of Publication V is that then, by using known relations between the eigenvalues and the network degrees d_i, the latter can be estimated to a good accuracy by solving a combinatorial problem; in fact, for, e.g., degree-regular networks, the correct degrees can always be found. Furthermore, should g be unknown, it is shown that this quantity can be estimated directly from the eigenfrequencies using graph theoretic arguments. While the scheme is illustrated with quantum networks with a Hamiltonian of the form (5.4), the results apply to any networks amenable to the extraction of the Laplace eigenvalues. In the case of non-uniform coupling strengths, estimation of the total interaction strengths of the oscillators with the rest of the network can be carried out, but this is less accurate as briefly discussed in the Publication V.

While it is possible to estimate the degree sequence just by having access to any single node of the network, the computational time it takes to produce the estimate from the probed eigenvalues scales at least exponentially in N, limiting the sizes of networks for which the full estimation can be done. As the exact mean and variance of the degree sequence can be found directly from the eigenfrequencies, bigger networks can still be classified accordingly. Since the estimate is constructed from all the possible solutions to the combinatorial problem, one could also consider using a reduced set of solutions to trade accuracy for speed.

5.2 Full access probing

In *full access probing*, no restrictions are imposed on the possible forms of $\mathbf{k}$. While one may still probe all of the quantities mentioned previously (in particular, the various spectral densities arising from different $\mathbf{g} = \mathbf{K}^\top \mathbf{k}$), in Publication I, it is shown that it is sufficient to be able to couple to single and pairs of nodes to reconstruct the full matrix $\mathbf{A}$ without making any assumptions on $\boldsymbol{\omega}$ or $\mathbf{L}$.

To begin, one may determine $\boldsymbol{\Omega}$ by local probing from any node. Consider next the system coupled to nodes l and m with the same interaction strength k, corresponding to $\mathbf{k}$ of the form $\mathbf{k}_i = (\delta_{il}+\delta_{im})k$. Then according to Eq. (4.2), probing reveals elements $g_i^2 = k^2(\mathbf{K}_{li} + \mathbf{K}_{mi})^2$. On the other hand, coupling to single node reveals the squared elements of a single row of $\mathbf{K}$. Consequently, probing N nodes individually followed by probing of

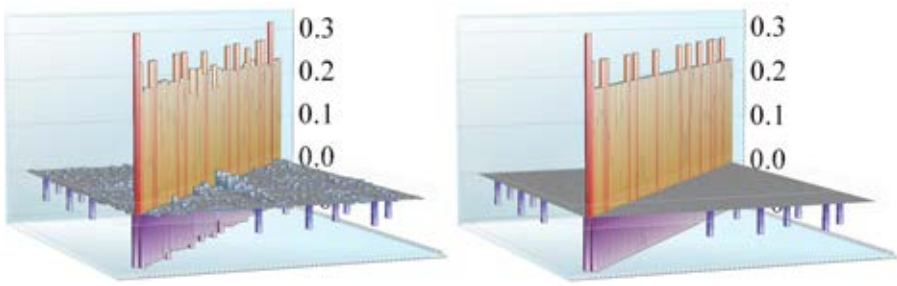

Figure 5.3: The detected matrix $\mathbf{A}$ (left), compared with the original (right) for a chain of 60 nodes with additional weak couplings. The initial state of the probe is squeezed vacuum with squeezing parameter $r = 1$ and phase-space angle $\phi = \pi/2$, while the network is initially in vacuum. The chain couplings and seven extra links have coupling strengths of $g = 0.2$ and $g/2$, respectively. Bare frequencies are $\omega_0 = 0.25$. This Figure has been reproduced from Publication I.

$N - 1$ pairs of nodes determines $\mathbf{K}$ save for an arbitrary global sign, since comparing, e.g., $\mathbf{K}_{li}^2 + \mathbf{K}_{mi}^2$ with $(\mathbf{K}_{li} + \mathbf{K}_{mi})^2$ reveals whether $\mathbf{K}_{li}$ and $\mathbf{K}_{mi}$ should have the same sign or not. As the global sign leaves $\mathbf{A} = \mathbf{K}\boldsymbol{\Delta}\mathbf{K}^\top$ invariant, then as far as $\mathbf{k}$ is considered, it is sufficient to couple to up to two nodes at once to determine $\mathbf{A}$.

An extra step which proved crucial in the simulations presented in Publication I was to enforce the orthogonality of the probed $\mathbf{K}$ through its singular value decomposition $\mathbf{K} = \mathbf{W}\boldsymbol{\Delta}\mathbf{V}$, since for any square matrix, $\mathbf{WV}$ is both orthonormal and near to the decomposed matrix in terms of the Frobenius norm [103]. An example is shown in Figure 5.3, where the network is a chain with several weak shortcuts.

To reconstruct $\mathbf{A}$ by determining each of the elements of the typically dense matrix $\mathbf{K}$, the total number of measurements scales as N^2 which makes this approach somewhat impractical. While it is conceivable that additional assumptions could help as it happens in the minimal access case, this was not investigated in the Publications introduced in this Thesis. Instead, in the following Section the network discrimination problem will be introduced and briefly discussed.

5.3 On network discrimination

Consider two quantum networks with N nodes but unknown matrix $\mathbf{A}$. What is the optimal way to reveal if two networks are isomorphic or not, in the sense that the Hamiltonians are the same up to relabeling the nodes, through probing? Before discussing the answer to this question, it should be stressed that this is straightforward to generalize to more than two networks: indeed, one simply needs to partition the given set of networks into subsets of isomorphic networks.

Since the sets of eigenfrequencies corresponding to two generic networks have no elements in common and the eigenfrequencies can be probed from any single node, it is convenient to start from them. Even a single frequency present in one but missing in the other is a strong indication that the networks are not isomorphic: with minimal access probing, this happens for isomorphic networks only in the rare case that some elements of $\mathbf{K}$ vanish. This can be checked as N is known. In any case, the number of measurements one must do to verify that two networks are not isomorphic is typically small and can be done with minimal access probing. If it is discovered that the eigenfrequencies all coincide, one might be tempted to conclude that the networks must be the same, but this is not the case due to the existence of isospectral graphs, i.e. non-isomorphic graphs with the same eigenvalues.

Consider now the case of discriminating between two isospectral but distinct networks; one should turn the attention to the coupling strengths $\mathbf{g}$. The goal of probing $\mathbf{g}$ is to check if they correspond to the same orthogonal matrix or not. While different sampling strategies might be considered, suppose that two full sets have been probed, one from each network, and both from a single node, revealing two rows of the respective orthogonal matrices but without signs. In principle, one could cycle through all 2^N possible signs for one of the rows while keeping those of the other fixed and see if the dot product becomes consistent with zero, but this number is prohibitively large for networks of any reasonable size, and in practice one would have to probe the signs as described previously. If the exhaustive search can be carried out and it is found that the vectors are never orthogonal, then they necessarily are rows from different orthogonal matrices and one can conclude that the networks are non-isomorphic.

If signs are found that make the vectors orthogonal, it is still not known if they indeed are, leaving the problem unresolved. This is still the case

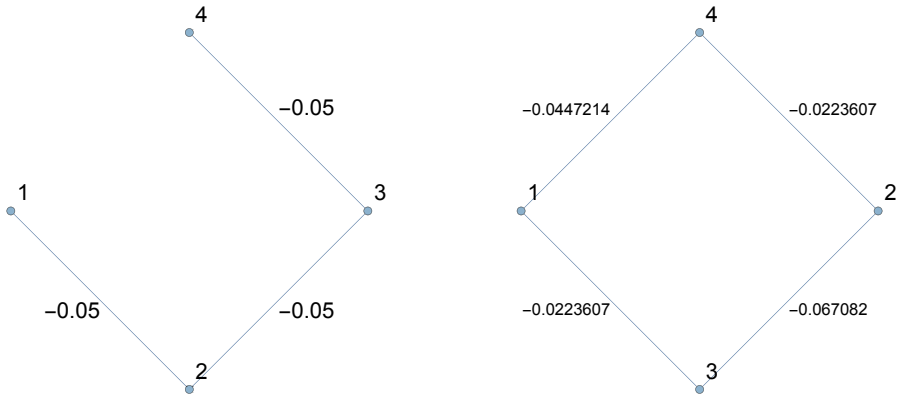

Figure 5.4: Two networks indistinguishable by probing with a coupling to (any) single node. The numbers shown next to the links correspond directly to the parameters of their respective Hamiltonians, while the nodes are labeled to emphasize that nodes adjacent in one might not be so in the other. The effective frequencies for both have a constant value $\tilde{\omega} = 0.12$. The indistinguishability is due to identical values of eigenfrequencies and squares of interaction strengths to normal modes when a probe is coupled to a node with the same label.

even when one has full knowledge of the eigenfrequencies and the signless matrices of both networks, as there exist non-isomorphic networks for which these quantities coincide.

To see this, note first that the number of orthogonal matrices consistent with the data one has is at least 2^{2n-1}, since orthogonality of rows and columns is preserved if an orthogonal matrix is multiplied from the left and right with diagonal matrices with each diagonal element ± 1. The claimed lower limit follows from the possible number of distinct pairs of such matrices; there can be more if the original matrix has duplicate or zero elements. Can these matrices, together with the eigenfrequencies, be an eigendecompositon of a matrix corresponding to a network non-isomorphic with the original? At least in some cases the answer is positive, such as in the examples shown in Fig. 5.4. Because of this, probing individually even all of the nodes is in general not enough, as the signs might have to be probed as well. Alternatively, one may settle for equivalence classes larger

than non-isomorphic networks. As a by-product, this also shows that in general, the ability to couple to single as well as pairs of nodes is not only sufficient but also necessary in the reconstruction of matrix $\mathbf{A}$. This holds even if multiple probes are used, since in minimal access case the coupling strengths to eigenmodes are directly proportional to a row of $\mathbf{K}$ for each probe, leaving the dynamics invariant with respect to the signs.

There are many open questions. For instance, the pair shown in the figure was found through exhaustive search starting from the chain, but the same search produced only isomorphic chains for any other length up to $N = 6$, raising the question whether having nontrivial counterparts is in fact rare. The standard next step would be to study the prevalence in ER networks, but for all but the smallest of cases, this would require more efficient computational approaches to make the problem tractable. If such sets could be found, it could be checked, e.g., how quantum walks on them differ. This problem should also be compared to the related problem of discrimination between two cluster states [104].

In conclusion, while it is typically easy to establish that given networks are distinct with just minimal access probing, verifying that networks are isomorphic appears to be nearly as challenging as probing their entire structure, and in general requires coupling the probe to two nodes at a time.

Chapter 6

Network mediated transport and routing

The first Section considers on the one hand how excitation transfer is affected by the network structure, and on the other hand how transport from an external system to the network can be effectively described when the interaction is weak. It will be discussed why the graph structure does not predict well how excitations will spread in complex networks, at variance with how excitations behave in lattices. The rest of the Chapter is an outlook for future work that will be further developed in the next months, dealing with a problem closely related to state transfer.

6.1 Transport of quantum information

In Section 4.2 it was seen that in some cases, merely changing a single link can drastically change the network spectral density $J(\omega)$. An example is given in Fig. 6.1, where a homogeneous chain with nearest and next nearest neighbor couplings is considered unaltered and with a single randomly chosen link rewired. An open system in a thermal state of $T = 1$ is coupled to an end of the chain in vacuum and is resonant with the chain $J(\omega)$, leading to exchange of excitations.

In the unaltered case, excitations propagate steadily in the chain. When the link is rewired, the dynamics is the same until the excitations reach a point affected by the rewiring. At this point, only a tiny fraction of excitations are able to continue along the chain. The rest are either reflected back towards the system or take the shortcut created by the rewired link and then proceed to propagate in both directions at the other end, leading

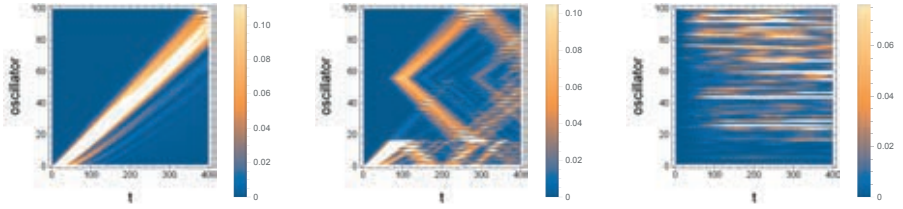

Figure 6.1: Examples of excitation transport in quantum networks. The color bar shows the difference between initial excitations and excitations at time t. On the left, the network is a homogeneous chain of $N = 100$ nodes with nearest and next nearest neighbor couplings with coupling strengths $g = 0.1$ and $g/5$, respectively, while the bare frequencies are set to $\omega_0 = 0.25$. Excitations propagate freely along the chain. In the middle, a single randomly chosen link in the chain has been rewired, changing the transport properties. On the right, evolution of excitations in the network oscillators of a random network of $N = 100$ oscillators with bare frequency $\omega_0 = 0.25$ and coupling strengths $g = 0.05$ is shown. Excitations become locked to a subset of network oscillators. Array values have been scaled for clarity. This Figure has been reproduced from Publication III.

eventually to a complicated pattern.

More generally, in lattices propagation is natural as the translational symmetry and often regularity of degrees both gives a natural scale to the network as the number of recurring subgraphs, and ensures that the effective frequencies are constant, making adjacent nodes always resonant with each other. This seems to make the underlying graph structure useful in predicting how excitations or information spread in the network. Consequently, it makes sense to consider a distance from the point of origin in the context of transport. The continuum regime characteristic for lattices discussed in Chapters 4 and 5 and exemplified in Figures 4.1 and 5.1 also plays an important role; it implies that even if the system frequency does not coincide with any eigenfrequency, the system is effectively resonant with the network up until t such that the oscillations in $\gamma(t)$ return.

A complex network is also depicted in the Fig. 6.1. The excitations do not spread out freely but instead seems to get locked into a subset of nodes. Unlike in the previous case, simply knowing which node is adjacent with

which does not seem to give much insight into how transport will happen, however what is observed could be explained by the interaction happening effectively with only a single eigenfrequency, as will be seen next.

If the system frequency coincides with some eigenfrequency Ω and interacts sufficiently weakly with the network, then to a good approximation the system interacts with only the resonant (possibly degenerate) eigenmode. Consequently, the dynamics should remain unaffected even if the coupling strengths to the other modes are set to 0. These effective couplings between the system and the eigenmodes can be expressed as

$$\mathbf{g}_{\text{eff}} = \mathbf{\Delta}_{\text{filter}}(\Omega)\mathbf{g} = \mathbf{\Delta}_{\text{filter}}(\Omega)\mathbf{K}^{\top}\mathbf{k}, \tag{6.1}$$

where the diagonal matrix $\mathbf{\Delta}_{\text{filter}}(\Omega)_{ii} = \delta_{\Omega_i\Omega}$ picks the elements of $\mathbf{g}$ corresponding to eigenmodes with frequency Ω. In the network basis the effective couplings read

$$\mathbf{k}_{\text{eff}} = \mathbf{K}\mathbf{g}_{\text{eff}} = \mathbf{K}\mathbf{\Delta}_{\text{filter}}(\Omega)\mathbf{K}^{\top}\mathbf{k}. \tag{6.2}$$

The effective couplings $\mathbf{k}_{\text{eff}}$ typically contain many non-vanishing elements even when the system is coupled to only one node. In other words, the open system is effectively coupled to many network nodes when resonant and the interaction is sufficiently weak. Network nodes cannot exchange excitations or quantum information with each other, as this would require interactions with multiple eigenmodes, and so excitations become locked as they do in the rightmost panel in Fig. 6.1.

It should be stressed that how strong the interaction strength can be before the system starts to interact in a non-negligible way with non-resonant eigenmodes can vary even when the network is fixed. This is essentially because it depends on how strong the interaction strength to the resonant eigenmode is relative to that of other eigenmodes in the vicinity of Ω and how close they are in terms of frequency. It may then happen that a given interaction strength with a single network node leads to interaction with just one eigenmode for certain frequencies only.

To see what kind of effective couplings can be engineered for a given frequency, one should consider the matrix acting on $\mathbf{k}$ in Eq. (6.2). The i-th column of this matrix (or equivalently, row, as the matrix is by con-

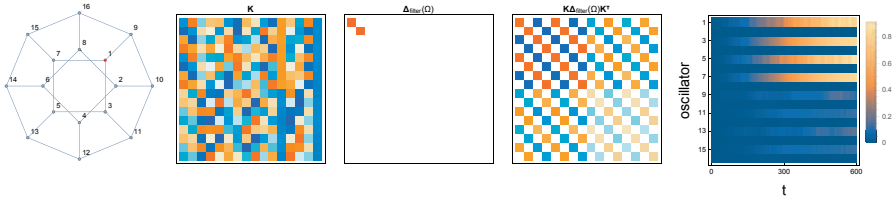

Figure 6.2: An example illustrating the relationship between the network, the effective couplings and transport. The orthogonal matrix $\mathbf{K}$ diagonalizes the network. In this particular case $\mathbf{\Delta}_{\text{filter}}(\Omega)$ contains multiple elements since the spectrum is degenerate. The matrix $\mathbf{K}\mathbf{\Delta}_{\text{filter}}(\Omega)\mathbf{K}^\top$ has a checkerboard pattern, predicting that no matter what is the point of contact, a weakly interacting system will be effectively decoupled from half of the network oscillators unless it is attached to multiple network nodes. On the other hand, coupling to, e.g., nodes 1 and 3 with equal weights leads to a complete decoupling since then all terms will cancel out. The rightmost panel corresponds to the system weakly coupled to node 1, leading to excitation exchange only with the nodes with an odd index.

struction symmetric) is directly proportional to $\mathbf{k}_{\text{eff}}$ when the system is directly coupled to i-th node, while different $\mathbf{k}$ lead to different weighted combinations.

A concrete example is given in Fig. 6.2. The network depicted in the leftmost panel has uniform coupling strengths $g = 0.15$ and constant bare frequencies $\omega_0 = 0.25$ and is initially in vacuum, while the system is in a thermal state with $\langle n(0)\rangle = 2$ and is coupled to node 1 with a coupling strength $k = 0.01$. The rightmost panel shows the change in node excitations.

In this particular case, it is seen that it is possible to choose $\mathbf{k}$ in such a way that the open system is effectively decoupled from the network. This can be achieved for example by coupling with identical strengths to nodes 1 and 3, as the corresponding terms in matrix $\mathbf{K}\mathbf{\Delta}_{\text{filter}}(\Omega)\mathbf{K}^\top$ will then cancel each other out. In terms of $\mathbf{g}$, this corresponds to the element belonging to the resonant eigenmode to cancel out, while other elements might remain non-zero. The checkerboard pattern of matrix $\mathbf{K}\mathbf{\Delta}_{\text{filter}}(\Omega)\mathbf{K}^\top$ implies that if the system is coupled weakly to any single network node it will be ef-

fectively decoupled from half of the network nodes. The rightmost panel confirms this as it shows that the system is able to exchange excitations only with the nodes with an odd index.

As they can predict how excitations will be distributed into the network, the effective couplings are considered as a tool to design networks with desired transport of excitations, quantum information and entanglement in upcoming work. Furthermore, it will be studied when the interaction with a single eigenmode is a valid assumption, which has implications also to the routing problem considered next.

6.2 The routing problem

The goal of state transfer on a network is to transfer a quantum state of a node marked as sender to another marked as receiver. In so called perfect state transfer, this is accomplished exactly, while sometimes pretty good state transfer is studied where the final state can be made to be arbitrarily close to the target state. In some cases this can be accomplished by the (lattice) structure alone, e.g., it is known that in a homogeneous chain of length 3, perfect state transfer between the end nodes can be accomplished by just the free Hamiltonian dynamics [26]. Alternatively, one may consider strategies suitable for more complex networks based on local control of the marked nodes only. The basic idea is to tune the marked nodes to be resonant with a suitable eigenmode of the rest of the network, such that the situation is effectively state transfer in a chain of three nodes. As the existence of such eigenmodes can be linked to eigenvalues of graph matrices, spectral graph theory can be of help; statistical results can be achieved by considering, e.g., generic spectra of ER graphs.

A problem closely related to the latter case will be the subject of upcoming work. Here, the eigenmodes of a network mediate state transfer between multiple external nodes, each having a corresponding interaction term of the form (4.2), such that states can be transferred between any pair of the external nodes and several pairs can exchange quantum information in parallel by using different available eigenmodes. The task is then to find suitable networks to this end. In this Thesis, this is called the *routing problem*, and the simultaneous exchange of quantum information through the network *routing*. Additionally it may be required that routing is achieved with reasonable speed and local control of the external nodes alone, i.e.

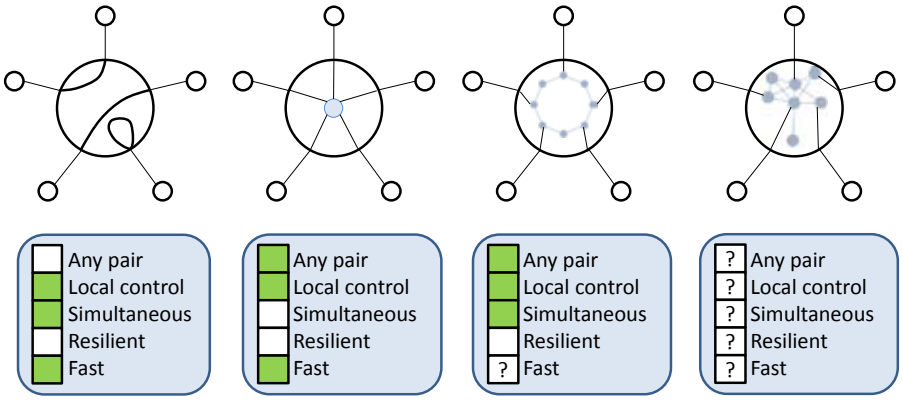

Figure 6.3: Several possible approaches to the routing problem are depicted and considered. Without a network, fast state transfer between fixed pairs is possible, requiring minimal control. Without the possibility for any pair to communicate and resilience to random node or link failures, this is unsatisfactory. The simplest possible network allows any pairs to communicate sequentially, but if the central node is lost communication becomes impossible. The ring is superior to the others, lacking only in resilience. Finally, complex networks are, as of yet, unknown area.

the network Hamiltonian can be static. Finding networks where such efficient routing is possible could have applications in, e.g., short-distance state transfer inside an apparatus processing quantum information. Such devices could then perhaps be used as building blocks in larger networks.

The problem as described has been considered previously, using a ring of nodes [105]. While otherwise a very viable approach, rings, and more generally lattices, have typically low vertex- and edge-connectivity, making them sensitive to random node or link failures. The ring, as well as some other possibilities are depicted and compared in Fig. 6.3. In the first case on the left, there is no network. Instead the external nodes are directly coupled to one another. Routing, as outlined earlier, cannot be done with this setup. The simplest possible network, i.e. a lone node, is somewhat better as by tuning the external oscillators in resonance with it, any pair can communicate. This solution is however neither capable of simultaneous transfer and therefore not useful for routing, nor is it resilient. Unlike the

toy solutions, the proposed ring can be used for routing and is lacking in resilience only. The transfer speed will depend on which modes are available. Finally, complex networks could be considered.

In the last case, the open questions are many. What kind of advantages, other than resilience, could complex networks have over lattices? Which networks are best? How should networks be compared and ranked based on their ability to route quantum information? What properties should be prioritized? What restrictions should be imposed? Partial answers will be provided in the next Section.

6.3 Network routing capacity

For a systematic search of networks suitable for routing, a figure of merit that allows for quick comparisons between them is needed. Tentatively, properties useful for such a quantity might include the following:

1. It should single out networks that have many eigenmodes suitable for state transfer.

2. The result should be a single real number with a clear interpretation.

3. The definition should be clear and physically motivated.

4. Evaluating it for a given network should have a computational complexity at most polynomial in N and the number of external nodes.

For the rest of this Section, this quantity, yet to be defined, is called *network routing capacity*.

The first item is clear. The second allows for sorting the networks according to their routing capacity, while also giving immediate and concise information about a given network to the user. The third is required for clarity and soundness, and should allow one to have more confidence in the results as opposed to an ad hoc definition. The last item has its drawbacks.

For communication through a network eigenmode to be possible for a given pair of external (input/output) nodes, at least one eigenmode must be suitable for both. Taking this into account would require checking all possible pairs of external nodes, forcing one to discard item 4. Considering the eigenmodes one external node at a time instead leads to significantly

more effective evaluation, but some relevant information is lost as the recipient side is ignored. Further assuming that the external nodes are coupled to a single network node implies that it is enough to consider each eigenvector separately, which leads to polynomial running time provided that a constant time is used for each element of each eigenvector. While a more complete picture would be obtained by taking into account both the sender and reciever as well as the possibility to couple to multiple network nodes, this would easily lead to a quantity too heavy to compute to be of practical use.

To understand better what should be taken into account, consider the situation depicted in Fig. 6.4. Here the focus is on a single eigenmode indexed i, and depicted are quantities that affect its usefulness for state transfer. For simplicity, only the nearest neighbors in terms of frequency are considered. Ratios x and y determine how the coupling strength g_i compares to its left and right neighbors; the closer these numbers are to 0 the better, as then g_i dominates over g_{i-1} and g_{i+1}. Consequently, the external node is more likely to interact only with eigenmode i. The magnitude of g_i itself should also be taken into account, as very low values will obviously reduce the usefulness of the eigenmode. Also shown are the differences between the mode frequency Ω_i and those of its neighbors; the larger these numbers are the better, as then the external node can more easily resolve the modes. For larger values, the external node can interact with the network with a stronger coupling while still interacting only with a single mode to a good approximation. Whether this particular mode is counted as suitable for transport should then be measured by some function f of the form $f(g_i, x, y, \Delta\Omega_{i-1,i}, \Delta\Omega_{i,i+1})$. Degenerate frequencies and the first and last frequencies having only a single neighbor should be accounted for in some appropriate manner.

To stay in line with item 2, the result of f could take binary values depending on whether the considered mode is counted or not. The extension to the entire network could then be simply the sum of the results over each of the N^2 possible elements of the eigenvectors; each eigenvector corresponds to a different point of contact in the network, while each element is associated with the frequency of the corresponding eigenmode. With these broad features, routing capacity of a network becomes a single positive integer, describing the total number of suitable modes when considering each of the network nodes separately as a point of contact.

The planned next steps are to consider how sensitive state transfer is to

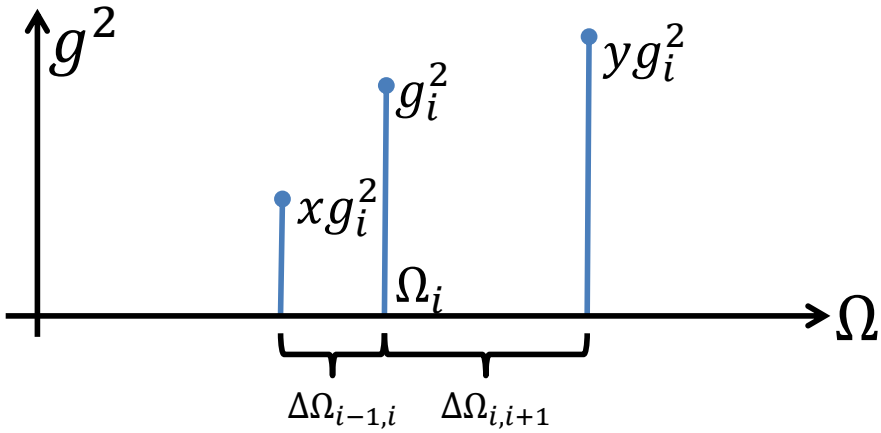

Figure 6.4: A simplified situation with three modes, where the suitability of the central one to routing is considered. The horizontal axis is frequency while the vertical one is the squared interaction strength of the corresponding mode with the external node. The depicted quantities affect transfer through the central mode. The rations x and y should be as small as possible and the distances $\Delta\Omega_{i-1,i}$ and $\Delta\Omega_{i,i+1}$ as large as possible for best results.

the four variables depicted in the simplified situation of Fig. 6.4, in order to find a suitable form for the function f. Then the routing capacity of networks complex enough to have a high vertex- and edge-connectivity will be benchmarked against that of lattices considered previously. A particular family of networks that will be tested are those based on a specific family of graphs with integer eigenvalues of the Laplace matrix, which should ensure that the eigenfrequencies are well separated from one another. The findings will be reported elsewhere.

Chapter 7

Experimental implementation of quantum networks

This Chapter focuses on physical implementations of complex quantum networks. The first Section discusses general features that can be expected to be applicable to a wide variety of models of quantum networks, while the second introduces an implementation of complex networks of quantum harmonic oscillators on a multimode optical platform from Publication IV.

7.1 Implementation generalities

Needless to say, often the requirements for efficient and flexible experimental implementations turn out to be system-dependent. Even after a system has been fixed, there may still be implementation-specific strengths, weaknesses and hurdles. This being said, considerations arising from the underlying graph structure are unique to networks. Implications of some broad features, such as the initial state of the network, are also discussed.

Structural considerations

Since even a single quantum harmonic oscillator would technically be a (trivial) quantum network, it is clear that the difficulty of implementing quantum networks will depend heavily on their structure. As far as connected networks are considered, implementing a connected network with N nodes requires a minimum of $N-1$ links (see Section 2.1), resulting in a

tree network. The simplest structure would be a chain of oscillators, which is not complex but can serve as a basis for more complicated networks. From here, one could either proceed to chains with non-uniform interaction strengths, or to random trees. In fact, provided that one has full control over the interaction strengths and oscillator frequencies, in principle any given spectral density can already be implemented with a chain (see Section 4.2), while tree networks tend to lead to highest non-Markovianity in the early reduced dynamics of an open quantum system (see Section 4.3). Both types of networks could tentatively be called complex for quantum networks, in the sense given in Section 2.2.

Starting instead from a ring or a grid of nodes would increase the required number of links while still requiring only short-range interactions. If at least some of the links could be rewired or additional long-range interactions could be engineered, one might consider the resulting network to be similar at least in spirit with the WS graphs, as the underlying regular structure could potentially result in a high transitivity while the added or rewired long-range links would reduce the network diameter. With enough of such shortcuts, the network could be called complex.

Having ER or BA networks could perhaps prove to be more difficult, as neither of them can be constructed from a regular or symmetric network. In particular, BA networks typically have a few nodes with a very high degree, which could pose a challenge. It may also be a requirement that the nodes of the network can be placed such that no links cross; this property is known as *planarity*. This could be satisfied by design with the previous examples but clearly not with generic ER or BA networks. Random graph models aside, the upper bound on the number of edges is given by a well-known corollary of Euler's formula: for simple connected planar graphs with $N \geq 3$ vertices and M edges, $M \leq 3N - 6$.

If many nodes are available, an alternative approach could perhaps be to partition the graph of the network into planar *subgraphs* (i.e., graphs composed of a subset of vertices and edges of a given graph), realize each subgraph separately and use long-range interactions only to join the corresponding nodes belonging to different subgraphs to effectively realize the network. The minimum number of such subgraphs is given by a property called graph *thickness*. An approach in such a spirit has been very recently proposed to improve quantum annealer designs through additional interactions that the authors refer to as small-world interactions [106].

The greatest challenge would be to implement networks complex also

from the classical point of view, such as quantum networks modeled after a real complex network. The reference networks typically used in network science literature range from the small $N = 34$ and $M = 78$ karate club social network [107] to massive $N \sim 10^5$ and $M \sim 10^6$ network of web pages within nd.edu domain constructed in late 1990s [108], and beyond. Assuming that the structure can be complex but size is restricted, one could still fabricate quantum networks useful for routing of quantum information (previous Chapter). At variance, large but significantly less complex networks could be useful for, e.g., implementing finite environments with a given spectral density (Chapter 4).

Implementation strategies

The desired state of the network, the degree of faithfulness to the theoretical model, and versatility of the implementation are crucial aspects somewhat separate from structure and size.

What the state of the network should be depends of course on the intended application. Vacuum would be a natural state to aim for when implementing networks to transfer or route quantum information, while a thermal state might be more suitable for a network intended to be an environment. To have dynamics that are hard to simulate on a classical computer, the inital state would have to be chosen accordingly; for an oscillator network, such a state would be non-Gaussian [83]. The ease or difficulty of preparing each of these sates is in general specific to the experiment.

An experimental implementation can be an emulation of the theoretical model, in the sense that the outward behavior matches that of the model in some sense, while the internal workings might differ. In other words, an emulation can substitute what it emulates. Suitable approaches will then depend on what features of the model will be focused on. For example, one might emulate a snapshot of the network dynamics, in the sense that measurement results in the experiment will correspond to those of the model at a given time, but the dynamics of the system emulating the network with respect to wall-clock time do not necessarily match that of the model. Alternatively, the real-time network dynamics could be emulated, either for a transient or for an extended period of time. The snapshot approach could be satisfactory for example for emulating dynamics that are hard or intractable to simulate on a classical computer, while the latter would be

needed to, e.g., implement quantum networks for routing as discussed in previous Chapter.

An implementation might be fixed, in the sense that readily changing the network is not possible but rather requires changing the experimental setup, or perhaps fabrication of a new network. Networks of mechanical oscillators and couplings can be expected to fall into this class. In contrast, a reconfigurable implementation would allow one to implement many networks in the same setup, ideally with full control of the number of nodes, links and structure. While appealing, reconfigurability may be hard to achieve with mechanical couplings between the nodes but can be done for example with nonlinear interactions between optical modes, as will be seen in the next Section.

7.2 Reconfigurable implementation of quantum complex networks

Specific systems are briefly considered as candidates for networks of quantum harmonic oscillators in Section 2.3 of Publication III. The basic requirements are repeated here: harmonic potential and quantum regime for the oscillators; static network structure; and springlike coupling between oscillators, with other interactions either minimized or eliminated. In Publication IV, a proposal is made to implement quantum networks using a multimode optical platform. As the proposal is heavily based on the considerable versatility of the platform, the core aspects will be briefly described here. A more in depth description may be found in Section 3 in Publication IV, as well as Refs. [109, 110] .

The initial quantum resource is a non-classical continuous variable photonic state. This state results from a simultaneous down-conversion of the components of a frequency comb produced by a mode-locked laser, e.g., a laser operated to produce pulses of an extremely short duration. Mode-selective measurements implemented using homodyne detection are performed on the optical modes to complete the protocol. The optical architecture being fixed, the spectral shapes of the frequency comb and the local oscillator used in the homodyne detection can be controlled. As will be seen, this setup is capable of producing quantum networks of moderate size and in principle arbitrary structure.

The comb consists of a very large number of frequency components,

which are simultaneously down-converted by a nonlinear optical element, namely a $\chi^{(2)}$ crystal, contained in a cavity. The down-conversion correlates each frequency component in the comb with every other. For these correlations to be preserved, the repetition rate of the comb must match the cavity free spectral range. When this condition is met, the device consisting of the pump laser, optical cavity and the crystal is called a synchronously pumped optical parametric oscillator.

The Hamiltonian of this process is

$$H_{\mathrm{ex}} = ig((\mathbf{a}^\dagger)^\top \boldsymbol{\mathcal{L}} \mathbf{a}^\dagger + \mathrm{h.c.}), \tag{7.1}$$

where $(\mathbf{a}^\dagger)^\top = \{a_1^\dagger, a_2^\dagger, \ldots\}$ is the vector of creation operators corresponding to the optical modes, $\boldsymbol{\mathcal{L}}$ is the matrix that describes how the modes are coupled, and g is a term regulating the overall interaction strength, proportional to the pump amplitude. Matrix $\boldsymbol{\mathcal{L}}$ has elements $\boldsymbol{\mathcal{L}}_{m,n} = f_{m,n} p_{m,n}$, where $f_{m,n}$ is the crystal's phase matching function and $p_{m,n}$ the pump amplitude at frequency $\omega_m + \omega_n$. The interaction leads to a similar amount of correlated down-converted frequencies than there was in the original spectrum.

Diagonalization of this Hamiltonian leads to an equivalent form $H_{\mathrm{ex}} = ig((\boldsymbol{\mathcal{A}}^\dagger)^\top \boldsymbol{\Delta}_{\mathrm{ex}}^{\mathrm{sq}} \boldsymbol{\mathcal{A}}^\dagger + \mathrm{h.c.})$, which describes uncorrelated squeezed modes, called supermodes, where each supermode in $\boldsymbol{\mathcal{A}}^\dagger$ is squeezed according to the corresponding element of the diagonal matrix $\boldsymbol{\Delta}_{\mathrm{ex}}^{\mathrm{sq}}$. The mode-selective measurements implement a basis change from the basis of the supermodes to measurement basis, given by a symplectic and orthogonal matrix $\mathbf{R}_{\mathrm{ex}}$. The total symplectic transformation, provided that the input modes are in the vacuum state, can then be written as

$$\mathbf{x}_f = \mathbf{R}_{\mathrm{ex}} \boldsymbol{\Delta}_{\mathrm{ex}}^{\mathrm{sq}} \mathbf{X}_{\mathrm{vac}}, \tag{7.2}$$

where $\mathbf{x}_f$ and $\mathbf{X}_{\mathrm{vac}}$ are the vectors of final and vacuum quadrature operators, respectively. The goal is to tune the matrices $\mathbf{R}_{\mathrm{ex}}$ and $\boldsymbol{\Delta}_{\mathrm{ex}}^{\mathrm{sq}}$ such that the resulting symplectic evolution matches that of the quantum network. To see what needs to be done, the symplectic matrix in Eq. (3.21) should be expressed in a similar form to that of Eq. (7.2). The former equation may be rewritten simply as $\mathbf{x}_f = \mathbf{S}(t)\mathbf{X}_i$, where $\mathbf{S}(t)$ is the symplectic matrix

encoding the network dynamics and $\mathbf{X}_i$ is the vector of initial quadrature operators.

To begin, the preparation of the initial Gaussian state is written in terms of a symplectic matrix $\mathbf{S}_0$ acting on the vacuum quadratures as $\mathbf{X}_i = \mathbf{S}_0\mathbf{X}_{\text{vac}}$. The product of this and the symplectic matrix giving the dynamics defines an effective symplectic matrix $\mathbf{S}_{\text{eff}} = \mathbf{S}(t)\mathbf{S}_0$. Substituting, the equation now reads $\mathbf{x}_f = \mathbf{S}_{\text{eff}}\mathbf{X}_{\text{vac}}$. Next, $\mathbf{S}_{\text{eff}}$ is written in terms of its Bloch-Messiah decomposition as $\mathbf{S}_{\text{eff}} = \mathbf{R}_1\mathbf{\Delta}^{\text{sq}}\mathbf{R}_2$. Substituting and remembering that vacuum is basis independent, i.e. $\mathbf{R}_2\mathbf{X}_{\text{vac}} = \mathbf{X}_{\text{vac}}$, the sought form is recovered as $\mathbf{x}_f = \mathbf{R}_1\mathbf{\Delta}^{\text{sq}}\mathbf{X}_{\text{vac}}$. The steps are summarized in Eq. (7.3) below:

$$\begin{aligned}\mathbf{x}_f &= \mathbf{S}(t)\mathbf{X}_i \\ &= \mathbf{S}(t)\mathbf{S}_0\mathbf{X}_{\text{vac}} \\ &= \mathbf{S}_{\text{eff}}\mathbf{X}_{\text{vac}} \\ &= \mathbf{R}_1\mathbf{\Delta}^{\text{sq}}\mathbf{R}_2\mathbf{X}_{\text{vac}} \\ &= \mathbf{R}_1\mathbf{\Delta}^{\text{sq}}\mathbf{X}_{\text{vac}}.\end{aligned} \tag{7.3}$$

Having the target matrices at hand, what remains is to match $\mathbf{R}_{\text{ex}}$ with $\mathbf{R}_1$ by shaping the local oscillator and $\mathbf{\Delta}^{\text{sq}}_{\text{ex}}$ with $\mathbf{\Delta}^{\text{sq}}$ by shaping the frequency comb. In the latter case, the relation between experimentally controllable parameters and the squeezing parameters in $\mathbf{\Delta}^{\text{sq}}_{\text{ex}}$ is in fact quite complicated, but the simulation results presented in Publication IV confirm that optimizing the parameters with heuristic methods [111] is both tractable and sufficient. By realizing the symplectic transformation of Eq. (7.3) in this way, the theoretical model is mapped to the experimental platform as summarized in Table 7.1, reproduced from Publication IV. The experiment emulates a snapshot of the network dynamics for a given point of time, and does so in a way that is reconfigurable to in principle arbitrary structure, as shown by simulation results using synthetic networks generated with the random graph models presented in Section 2.2, as well as real complex networks. Having networks with tens of nodes is within reach.

An example of such simulation results is shown in Fig. 7.1, where the probing of the spectral density (see Sections 4.1 and 5.1) is simulated for two synthetic and two real complex networks, with the probe in squeezed

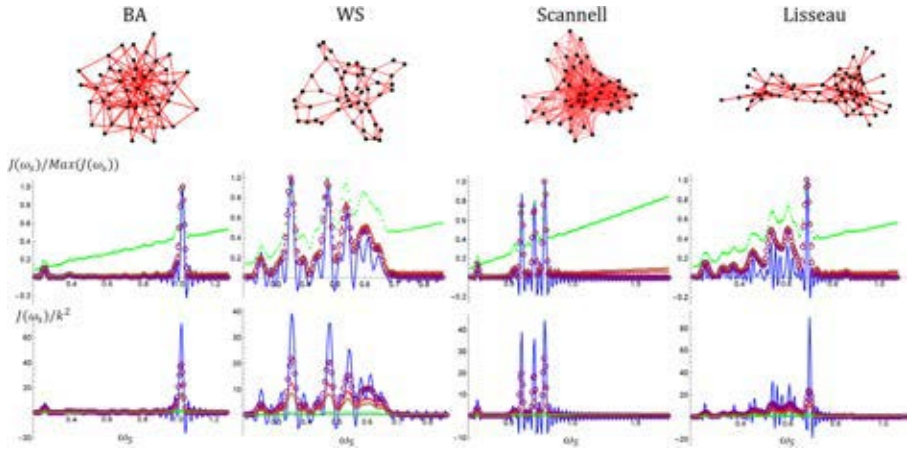

Figure 7.1: Simulation of the probing of the spectral density with the experimental platform. The columns correspond to the used networks. The Scannell network is a connectome [112] while the Lisseau network is a social network [113]. Blue lines and violet circles are the spectral densities and probed values, as in Fig 5.1. Green dots correspond to $\mathbf{\Delta}_{\mathrm{ex}}^{\mathrm{sq}}$ obtained without pump optimization. The red and brown dots correspond to optimized pump shapes for nonlinear crystal lengths of 1.5 and 0.5 mm, respectively. Middle row: the probed values are normalized with respect to the maximum value of the spectral density. Bottom row: the results without normalization. This Figure has been modified from figures of Publication IV.

state and the network in vacuum. The good match with expected results confirms that the dynamics is able to mimic the one of the model for a wide range of values of the probe frequency. The squeezing parameters encoded in $\mathbf{\Delta}^{\mathrm{sq}}$ tend to be of small magnitude in this scenario, except for the one corresponding to the probe, while optimized pump shape tends to lead to some squeezing of all modes, as seen in Fig. 7.2. This will decrease the energy difference between the probe and the network from the assumed value, leading to probed values of the spectral density to be smaller than those expected in the simulations; scaling the probed values confirms that the correct structure is recovered to a good accuracy, however, as seen in the middle row of Fig. 7.1. Comparing the results shown here and in, e.g., Fig. 10 in Publication IV shows that the importance of the optimization of

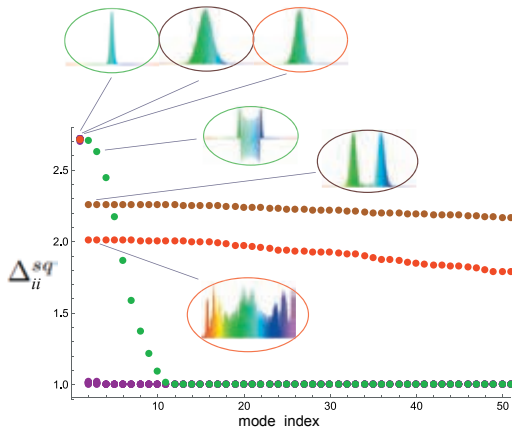

Figure 7.2: Purple: diagonal elements of the target $\mathbf{\Delta}^{\mathrm{sq}}$; green: experimentally achievable squeezing spectrum without pump shape optimization, i.e. diagonal elements of $\mathbf{\Delta}_{\mathrm{ex}}^{\mathrm{sq}}$ in the case of a Gaussian pump spectrum for the parametric process with a crystal length of 1.5 mm. Brown and red: experimentally achievable squeezing spectrum with pump shape optimization with a nonlinear crystal length of 0.5 and 1.5 mm. In the three cases (green, red and brown) the first diagonal element matches the target exactly (purple). The pictures in the circles show the spectral shapes of the first and the third modes in the three possible experimental configurations. This Figure has been reproduced from Publication IV.

the comb shape becomes more important as the complexity of the networks increases.

Further improvements could be possible by considering the state of the network to be approximately squeezed instead of the vacuum, as in practice optimization tends to lead to squeezing of the supermodes. Alternatively, one could consider the possibility of using auxiliary supermodes which would receive the squeezing, instead of the supermodes that will be used to build the network. This could potentially make the implementation more flexible in terms of target squeezing parameters, as the particular squeezing profile of the auxiliary modes would not matter.

	Quantum network	Experimental implementation
Node	Quantum harmonic oscillator	Optical mode
Link	Spring-like coupling term	Nonlinear mode coupling
t	Wall-clock time	Parameter controlling the symplectic matrix $\mathbf{R}_{\mathrm{ex}}\mathbf{\Delta}_{\mathrm{ex}}^{\mathrm{sq}}$
Frequency	Oscillator frequencies	Squeezing of optical modes
Decoupled mode	Normal mode of the network	Supermode, a non-correlated squeezed optical mode
Addressing a node	Local measurement	Pulse shaping & mode-selective measurement of the supemodes

Table 7.1: The mapping of the quantum networks to the experimental platform. Refer to main text and Publication IV for more details. This Table has been reproduced from Publication IV.

Chapter 8

Conclusions

This Thesis provides an introductory overview of the main results of the Publications I-V authored by the PhD student Johannes Nokkala. The results concern complex networks of interacting quantum harmonic oscillators in the case of exact Gaussian dynamics. To make the thesis more self-contained, a brief introduction to the still developing field of quantum networks is also provided.

A key quantity considered in Chapter 4 is the network spectral density. In Publication I, it is shown how the network structure affects the spectral density and how it can be shaped in a controllable manner by making small changes in the network structure. It is well known how an in principle arbitrary spectral density can be realized with a finite set of non-interacting modes, or alternatively with a chain of oscillators with nearest neighbor interactions only. In this Thesis, the more general problem of simultaneously realizing several given spectral densities with a single component network is briefly considered and the possibilities and limitations are discussed. The non-Markovianity of the reduced dynamics of an open system in contact with a network is also considered. In Publication II, the spectral density is fixed and non-Markovianity is compared with the backflow of excitations, also in the strong coupling regime. It is shown that, unlike in the case of a fermionic bath [98], excitation backflow is not tied to non-Markovianity. In Publication III it is shown that, on average, increasing the density of links in a complex network tends to suppress non-Markovianity in the early and intermediate reduced dynamics.

The complementary point of view is taken in Chapter 5, where it is studied which information about a complex network can be extracted by monitoring the reduced dynamics of a controllable open system interacting with it. In Publication V, results from spectral graph theory are leveraged

to develop a local probe for the degree sequence and coupling strength for networks of identical oscillators and uniform interaction strengths. It is shown that access to any single node of the network is sufficient. It should be mentioned that the results are applicable to any networks, quantum or classical, when one can probe the Laplace eigenvalues. Probing is also considered in Publication I, but without making any assumptions about the oscillator frequencies or the interaction strengths between them. From a single node access, the spectral density, eigenfrequencies and coupling strengths to eigenmodes can be extracted. With full access, in principle the entire structure can be extracted but this is costly. Because of this, in this Thesis the related problem of being able to discriminate between two networks is considered. It is shown that there are networks that cannot be discriminated even with full access, if the probe is coupled to only one node at a time.

In Chapter 6, the network acts as a mediator of quantum information transfer between multiple parties that each have full control over a quantum system coupled to a single network node. The impact of the network structure to transport properties was briefly considered in Publication III, and will be investigated in more detail in upcoming work where the routing capacity of a quantum network will be introduced and used to search for classes of complex networks with both high routing capacity and high resilience against random node or link failures.

Realizing a quantum network experimentally is always demanding, and in particular achieving a reasonable size and complex structure simultaneously poses a great challenge. In Chapter 7, these requirements are discussed and an introduction to the results from Publication IV is provided. In this work, a proposal for an experimental implementation of quantum complex networks is made. It is based on mapping the network dynamics to a multimode optical platform. A key strength of this proposal is reconfigurability, i.e. the ability to implement networks of in principle arbitrary structure, without changing the optical architecture. The versatility of the proposal is illustrated by simulating the probing of the spectral density (Publication I) of several networks, including ones with the structure of real complex networks.

The results of this thesis extend the existing studies on Hamiltonian-based quantum networks towards ones with a genuinely complex structure. In particular, the results deepen the understanding of the interplay between network structure and the non-Markovianity it can induce in the reduced

dynamics of an open quantum system. The Thesis introduces several new tools to probe quantum networks, with the method to probe the spectral density applicable also to heat baths with a continuum of frequencies. The Thesis advances experimental network theory by introducing the first proposal to implement networks with in principle arbitrary structure in a fully reconfigurable way. Finally, the introductory parts of the Thesis may inspire further research on quantum networks and encourage crosstalk and exchange of novel ideas between researchers working on different types of quantum networks, or even between researchers working on classical and quantum networks.

On the other hand, the possibilities offered by tuning individually the coupling strengths and bare frequencies were not fully explored. There are also many more complex network models that could have been used, while the benefits of complexity were only briefly discussed. This, together with restricting to Gaussian dynamics of closed networks leaves room for further work.

Indeed, by introducing the framework and introducing a host of interesting results, this Thesis has created a fertile ground for future research on quantum complex networks. One might continue to investigate the engineering aspect further to find networks beneficial for quantum information processing tasks, perhaps in the case of open networks and through induced non-Markovianity. Probing of networks could be investigated further by trying to apply optimal quantum estimation theory, like has been recently done for estimating parameters of an Ohmic structured reservoir characterized by its spectral density and temperature [99–101], or considering probing when partial knowledge of the network is available. Another possible research avenue would be to properly explore how and when structural complexity can be a useful resource. This can be expected to play a role in the upcoming work on routing of quantum information with quantum networks. Perhaps the most interesting future prospect would be to consider the experimental implementation of non-Gaussian dynamics of quantum networks, as this could potentially lead to experiments emulating quantum dynamics that is hard to classically simulate.

Bibliography

[1] E. Schrödinger. An undulatory theory of the mechanics of atoms and molecules. *Phys. Rev.*, 28:1049, 1926.

[2] W. Pauli. Über das wasserstoffspektrum vom standpunkt der neuen quantenmechanik. *Z. Phys.*, 36(5):336, 1926.

[3] W. Heitler and F. London. Wechselwirkung neutraler atome und homöopolare bindung nach der quantenmechanik. *Z. Phys.*, 44(6-7):455, 1927.

[4] P. A. M. Dirac. The quantum theory of the electron. *Proc. R. Soc. Lond. A.*, 117:610, 1928.

[5] P. A. M. Dirac. A theory of electrons and protons. *Proc. R. Soc. Lond. A.*, 126:360, 1930.

[6] W. Heisenberg and W. Pauli. Zur quantendynamik der wellenfelder. *Z. Phys.*, 56(1-2):1, 1929.

[7] W. Heisenberg and W. Pauli. Zur quantendynamik der wellenfelder. ii. *Z. Phys.*, 59(3-4):168, 1930.

[8] H. A. Bethe. The electromagnetic shift of energy levels. *Phys. Rev.*, 72(4):339, 1947.

[9] J. Schwinger. On quantum-electrodynamics and the magnetic moment of the electron. *Phys. Rev.*, 73(4):416, 1948.

[10] R. P. Feynman. Mathematical formulation of the quantum theory of electromagnetic interaction. *Phys. Rev.*, 80(3):440, 1950.

[11] T. H. Maiman. Stimulated optical radiation in ruby. *Nature*, 187:493 EP, 1960.

[12] R. J. Glauber. The quantum theory of optical coherence. *Phys. Rev.*, 130(6):2529, 1963.

[13] R. J. Glauber. Quantum optics. In *Quantum Optics*, 1969.

[14] R. S. Ingarden. Quantum information theory. *Rep. Math. Phys.*, 10(1):43, 1976.

[15] P. Benioff. The computer as a physical system: A microscopic quantum mechanical hamiltonian model of computers as represented by turing machines. *J. Stat. Phys.*, 22(5):563, 1980.

[16] R. P. Feynman. Simulating physics with computers. *Int. J. Theor. Phys.*, 21(6-7):467, 1982.

[17] D. Deutsch. Quantum theory, the church–turing principle and the universal quantum computer. *Proc. R. Soc. Lond. A*, 400(1818):97, 1985.

[18] S. Abramsky and B. Coecke. A categorical semantics of quantum protocols. In *Logic in computer science, 2004. Proceedings of the 19th Annual IEEE Symposium on*, page 415. IEEE, 2004.

[19] R. Albert and A.-L. Barabási. Statistical mechanics of complex networks. *Rev. Mod. Phys.*, 74(1):47, 2002.

[20] E. Alm and A. P. Arkin. Biological networks. *Curr. Opin. Struct. Biol.*, 13(2):193, 2003.

[21] J. Scott. *Social network analysis*. Sage, 2017.

[22] M. Epping, H. Kampermann, and D. Bruß. Large-scale quantum networks based on graphs. *New J. Phys.*, 18(5):053036, 2016.

[23] R. Raussendorf, D. E. Browne, and H. J. Briegel. Measurement-based quantum computation on cluster states. *Phys. Rev. A*, 68(2):022312, 2003.

[24] S. E. Venegas-Andraca. Quantum walks: a comprehensive review. *Quantum Inf. Process.*, 11(5):1015, 2012.

[25] A. M. Childs. Universal computation by quantum walk. *Phys. Rev. Lett.*, 102(18):180501, 2009.

[26] M. Christandl, N. Datta, A. Ekert, and A. J. Landahl. Perfect state transfer in quantum spin networks. *Phys. Rev. Lett.*, 92(18):187902, 2004.

[27] M. B. Plenio and S. F. Huelga. Dephasing-assisted transport: quantum networks and biomolecules. *New J. Phys.*, 10(11):113019, 2008.

[28] T. Scholak, F. de Melo, T. Wellens, F. Mintert, and A. Buchleitner. Efficient and coherent excitation transfer across disordered molecular networks. *Phys. Rev. E*, 83(2):021912, 2011.

[29] J. Nokkala, F. Galve, R. Zambrini, S. Maniscalco, and J. Piilo. Complex quantum networks as structured environments: engineering and probing. *Sci. Rep.*, 6:26861, 2016.

[30] G. Manzano, F. Galve, G. L. Giorgi, E. Hernández-García, and R. Zambrini. Synchronization, quantum correlations and entanglement in oscillator networks. *Sci. Rep.*, 3:1239, 2013.

[31] R. J. Wilson. *Introduction to Graph Theory (5th Edition).* Pearson (London), 2010.

[32] M. Newman. *Networks: an introduction.* Oxford university press, 2010.

[33] G. Bianconi. Interdisciplinary and physics challenges of network theory. *EPL*, 111:56001, 2015.

[34] J. Biamonte, M. Faccin, and M. De Domenico. Complex networks: from classical to quantum. *arXiv preprint arXiv:1702.08459*, 2017.

[35] A.-L. Barabási. *Network science.* Cambridge university press, 2016.

[36] A.-L. Barabási. Scale-free networks: a decade and beyond. *Science*, 325(5939):412, 2009.

[37] S. Chakraborty, L. Novo, A. Ambainis, and Y. Omar. Spatial search by quantum walk is optimal for almost all graphs. *Phys. Rev. Lett.*, 116(10):100501, 2016.

[38] C. Heunen, M. Sadrzadeh, and E. Grefenstette. *Quantum physics and linguistics: a compositional, diagrammatic discourse.* Oxford University Press, 2013.

[39] H. J. Briegel, D. E. Browne, W. Dür, R. Raussendorf, and M. Van den Nest. Measurement-based quantum computation. *Nat. Phys.*, 5(1):19, 2009.

[40] S. Anders and H. J. Briegel. Fast simulation of stabilizer circuits using a graph-state representation. *Phys. Rev. A*, 73(2):022334, 2006.

[41] N. C. Menicucci, S. T. Flammia, and P. van Loock. Graphical calculus for gaussian pure states. *Phys. Rev. A*, 83:042335, 2011.

[42] M. Faccin, T. Johnson, J. Biamonte, S. Kais, and P. Migdał. Degree distribution in quantum walks on complex networks. *Phys. Rev. X*, 3:041007, 2013.

[43] Z. Zimboras, M. Faccin, Z. Kadar, J. D. Whitfield, B. P. Lanyon, and J. Biamonte. Quantum transport enhancement by time-reversal symmetry breaking. *Sci. Rep.*, 3:2361, 2013.

[44] D. Lu, J. D. Biamonte, J. Li, H. Li, T. H. Johnson, V. Bergholm, M. Faccin, Z. Zimborás, R. Laflamme, J. Baugh, and S. Lloyd. Chiral quantum walks. *Phys. Rev. A*, 93(4):042302, 2016.

[45] G. M. Nikolopoulos and I. Jex. *Quantum state transfer and network engineering*. Springer, 2014.

[46] G. Mahler and R. Wawer. Quantum networks: dynamics of open nanostructures. *VLSI Design*, 8(1-4):191, 1998.

[47] E. Romero, R. Augulis, V. I. Novoderezhkin, M. Ferretti, J. Thieme, D. Zigmantas, and R. Van Grondelle. Quantum coherence in photosynthesis for efficient solar-energy conversion. *Nat. Phys.*, 10(9):676, 2014.

[48] D. Burgarth and K. Maruyama. Indirect hamiltonian identification through a small gateway. *New J. Phys.*, 11(10):103019, 2009.

[49] T. Tufarelli, A. Ferraro, M. S. Kim, and S. Bose. Reconstructing the quantum state of oscillator networks with a single qubit. *Phys. Rev. A*, 85(3):032334, 2012.

[50] D. Tamascelli, C. Benedetti, S. Olivares, and M. G. A. Paris. Characterization of qubit chains by feynman probes. *Phys. Rev. A*, 94(4):042129, 2016.

[51] J. Nokkala, S. Maniscalco, and J. Piilo. Local probe for connectivity and coupling strength in quantum complex networks. *Sci. Rep.*, 8(1):13010, 2018.

[52] M. Razavi. *An Introduction to Quantum Communication Networks: Or, How Shall We Communicate in the Quantum Era?* Morgan & Claypool Publishers, 2018.

[53] A. Reiserer and G. Rempe. Cavity-based quantum networks with single atoms and optical photons. *Rev. Mod. Phys.*, 87(4):1379, 2015.

[54] C.-Z. Peng et al. Experimental free-space distribution of entangled photon pairs over 13 km: towards satellite-based global quantum communication. *Phys. Rev. Lett.*, 94(15):150501, 2005.

[55] J.-Y. Wang et al. Direct and full-scale experimental verifications towards ground–satellite quantum key distribution. *Nat. Photonics*, 7(5):387, 2013.

[56] S.-K. Liao et al. Satellite-to-ground quantum key distribution. *Nature*, 549:43, 2017.

[57] H. J. Kimble. The quantum internet. *Nature*, 453(7198):1023, 2008.

[58] R. Beals, S. Brierley, O. Gray, A. W. Harrow, S. Kutin, N. Linden, D. Shepherd, and M. Stather. Efficient distributed quantum computing. *Proc. R. Soc. A*, 469(2153):20120686, 2013.

[59] J. I. Cirac, P. Zoller, H. J. Kimble, and H. Mabuchi. Quantum state transfer and entanglement distribution among distant nodes in a quantum network. *Phys. Rev. Lett.*, 78(16):3221, 1997.

[60] L. Aolita, A. J. Roncaglia, A. Ferraro, and A. Acín. Gapped two-body hamiltonian for continuous-variable quantum computation. *Phys. Rev. Lett.*, 106(9):090501, 2011.

[61] A. A. Ezhov and D. Ventura. Quantum neural networks. In *Future directions for intelligent systems and information sciences*, page 213. Springer, 2000.

[62] J. Gough and M. R. James. Quantum feedback networks: Hamiltonian formulation. *Commun. Math. Phys.*, 287(3):1109, 2009.

[63] A. Acín, J. I. Cirac, and M. Lewenstein. Entanglement percolation in quantum networks. *Nat. Phys.*, 3(4):256, 2007.

[64] P. J. Cameron, A. Montanaro, M. W. Newman, S. Severini, and A. Winter. On the quantum chromatic number of a graph. *Electron. J. Comb.*, 14(1):81, 2007.

[65] V. Danos and E. Kashefi. Determinism in the one-way model. *Phys. Rev. A*, 74(5):052310, 2006.

[66] B. Zeng, H. Chung, A. W. Cross, and I. L. Chuang. Local unitary versus local clifford equivalence of stabilizer and graph states. *Phys. Rev. A*, 75:032325, 2007.

[67] C. Gokler, S. Lloyd, P. Shor, and K. Thompson. Efficiently controllable graphs. *Phys. Rev. Lett.*, 118(26):260501, 2017.

[68] M. Krenn, X. Gu, and A. Zeilinger. Quantum experiments and graphs: Multiparty states as coherent superpositions of perfect matchings. *Phys. Rev. Lett.*, 119:240403, 2017.

[69] T. P. Le, L. Donati, S. Severini, and F. Caruso. How to suppress dark states in quantum networks and bio-engineered structures. *J. Phys. A.*, 51(36):365306, 2018.

[70] A. Ambainis and R. Špalek. Quantum algorithms for matching and network flows. In *Annual Symposium on Theoretical Aspects of Computer Science*, page 172. Springer, 2006.

[71] E. D'Hondt. Quantum approaches to graph colouring. *Theor. Comput. Sci.*, 410(4-5):302, 2009.

[72] S. Lloyd, S. Garnerone, and P. Zanardi. Quantum algorithms for topological and geometric analysis of data. *Nat. Commun.*, 7:10138, 2016.

[73] W.-L. Chang, Q. Yu, Z. Li, J. Chen, X. Peng, and M. Feng. Quantum speedup in solving the maximal-clique problem. *Phys. Rev. A*, 97(3):032344, 2018.

[74] A. Ferraro, S. Olivares, and M. G. A. Paris. Gaussian states in continuous variable quantum information. *Napoli Series on physics and Astrophysics*, 2005.

[75] H.-P. Breuer and F. Petruccione. *The Theory of Open Quantum Systems*. Oxford University Press, New York, New York, 2007.

[76] U. Weiss. *Quantum Dissipative Systems*. World Scientific, 4th edition, 2012.

[77] Y. Ticochinsky. On the diagonalization of the general quadratic hamiltonian for coupled harmonic oscillators. *J. Math. Phys.*, 20:406, 1979.

[78] M. B. Plenio, J. Hartley, and J. Eisert. Dynamics and manipulation of entanglement in coupled harmonic systems with many degrees of freedom. *New J. Phys.*, 6:36, 2004.

[79] J. Williamson. On the algebraic problem concerning the normal forms of linear dynamical systems. *Am. J. Math.*, 58(1):141, 1936.

[80] R. L. Hudson. When is the wigner quasi-probability density non-negative? *Rep. Math. Phys.*, 6(2):249, 1974.

[81] N. Lütkenhaus and S. M. Barnett. Nonclassical effects in phase space. *Phys. Rev. A*, 51(4):3340, 1995.

[82] S. L. Braunstein. Squeezing as an irreducible resource. *Phys. Rev. A*, 71(5):055801, 2005.

[83] S. D. Bartlett, B. C. Sanders, S. L. Braunstein, and K. Nemoto. Efficient classical simulation of continuous variable quantum information processes. *Phys. Rev. Lett.*, 88:097904, 2002.

[84] Y.-S. Ra, C. Jacquard, A. Dufour, C. Fabre, and N. Treps. Tomography of a mode-tunable coherent single-photon subtractor. *Phys. Rev. X*, 7:031012, Jul 2017.

[85] M. Walschaers, C. Fabre, V. Parigi, and N. Treps. Entanglement and wigner function negativity of multimode non-gaussian states. *Phys. Rev. Lett.*, 119:183601, Oct 2017.

[86] U. Chabaud, T. Douce, D. Markham, P. van Loock, E. Kashefi, and G. Ferrini. Continuous-variable sampling from photon-added or photon-subtracted squeezed states. *Phys. Rev. A*, 96:062307, Dec 2017.

[87] R.J. Rubin. Momentum autocorrelation functions and energy transport in harmonic crystals containing isotopic defects. *Phys. Rev.*, 131:964, 1963.

[88] A. O. Caldeira and A. J. Leggett. Path integral approach to quantum brownian motion. *Physica A*, 121(3):587, 1983.

[89] D. Chruściński and A. Kossakowski. Non-markovian quantum dynamics: local versus nonlocal. *Phys. Rev. Lett.*, 104(7):070406, 2010.

[90] E.-M. Laine, K. Luoma, and J. Piilo. Local-in-time master equations with memory effects: applicability and interpretation. *J. Phys. B*, 45(15):154004, 2012.

[91] H.-P. Breuer, E.-M. Laine, J. Piilo, and B. Vacchini. Colloquium: Non-markovian dynamics in open quantum systems. *Rev. Mod. Phys.*, 88(2):021002, 2016.

[92] I. de Vega and D. Alonso. Dynamics of non-markovian open quantum systems. *Rev. Mod. Phys.*, 89:015001, 2017.

[93] M. A. de Ponte, M. C. de Oliveira, and M. H. Y. Moussa. Decoherence in a system of strongly coupled quantum oscillators. i. symmetric network. *Phys. Rev. A*, 70:022324, 2004.

[94] M. A. de Ponte, M. C. de Oliveira, and M. H. Y. Moussa. Decoherence in a system of strongly coupled quantum oscillators. ii. central-oscillator network. *Phys. Rev. A*, 70:022325, 2004.

[95] B. Bellomo, G. L. Giorgi, G. M. Palma, and R. Zambrini. Quantum synchronization as a local signature of super- and subradiance. *Phys. Rev. A*, 95:043807, 2017.

[96] A. S. Householder. Unitary triangularization of a nonsymmetric matrix. *J. ACM*, 5(4):339, 1958.

[97] L. A. M. Souza, H. S. Dhar, M. N. Bera, P. Liuzzo-Scorpo, and G. Adesso. Gaussian interferometric power as a measure of continuous-variable non-markovianity. *Phys. Rev. A*, 92(5):052122, 2015.

[98] G. Guarnieri, C. Uchiyama, and B. Vacchini. Energy backflow and non-markovian dynamics. *Phys. Rev. A*, 93:012118, 2016.

[99] M. Bina, . Grasselli, and M. G. A. Paris. Continuous-variable quantum probes for structured environments. *Phys. Rev. A*, 97:012125, Jan 2018.

[100] C. Benedetti, F. Salari Sehdaran, M. H. Zandi, and M. G. A. Paris. Quantum probes for the cutoff frequency of ohmic environments. *Phys. Rev. A*, 97:012126, Jan 2018.

[101] S. Razavian, C. Benedetti, M. Bina, Y. Akbari-Kourbolagh, and M. G. A. Paris. Quantum thermometry by single-qubit dephasing. *arXiv preprint arXiv:1807.11810*, 2018.

[102] S. Maniscalco, J. Piilo, F. Intravaia, F. Petruccione, and A. Messina. Simulating quantum brownian motion with single trapped ions. *Physical Review A*, 69(5):052101, 2004.

[103] N. J. Higham. Computing the polar decomposition—with applications. *SIAM J. Sci. Comput.*, 7(4):1160, 1986.

[104] S. Bandyopadhyay, S. Halder, and M. Nathanson. Optimal resource states for local state discrimination. *Phys. Rev. A*, 97(2):022314, 2018.

[105] S. Paganelli, S. Lorenzo, T. J. G. Apollaro, F. Plastina, and G. L. Giorgi. Routing quantum information in spin chains. *Phys. Rev. A*, 87(6):062309, 2013.

[106] H. G. Katzgraber and M. A. Novotny. A small-world search for quantum speedup: How small-world interactions can lead to improved quantum annealer designs. *arXiv preprint arXiv:1805.09510*, 2018.

[107] W. W. Zachary. An information flow model for conflict and fission in small groups. *J. Anthropol. Res.*, 33(4):452, 1977.

[108] R. Albert, H. Jeong, and A.-L. Barabási. Internet: Diameter of the world-wide web. *Nature*, 401(6749):130, 1999.

[109] J. Roslund, R. M. de Araújo, S. Jiang, C. Fabre, and N. Treps. Wavelength-multiplexed quantum networks with ultrafast frequency combs. *Nat. Photonics*, 8:109, 2013.

[110] R. Medeiros de Araújo, J. Roslund, Y. Cai, G. Ferrini, C. Fabre, and N. Treps. Full characterization of a highly multimode entangled state embedded in an optical frequency comb using pulse shaping. *Phys. Rev. A*, 89:053828, 2014.

[111] F. Arzani, C. Fabre, and N. Treps. Versatile engineering of multimode squeezed states by optimizing the pump spectral profile in spontaneous parametric down-conversion. *Phys. Rev. A*, 97:033808, 2018.

[112] J. Scannell, G. Burns, C. Hilgetag, M. O'Neil, and M. Young. The connectional organization of the cortico-thalamic system of the cat. *Cereb. Cortex*, 9(3):277, 1999.

[113] D. Lusseau, K. Schneider, O. J. Boisseau, P. Haase, E. Slooten, and S. M. Dawson. The bottlenose dolphin community of doubtful sound features a large proportion of long-lasting associations. *Behav. Ecol. Sociobiol.*, 54(4):396, 2003.

Annales Universitatis Turkuensis

UNIVERSITY OF TURKU

ISBN 978-951-29-7467-2 (PRINT)
ISBN 978-951-29-7468-9 (PDF)
ISSN 0082-7002 (Print) ISSN 2343-3175 (Online)

Grano Oy, Turku, Finland 2018